CERN-PH-TH/2012-234

Testing Lorentz invariance of dark matter

Diego Blas[a*], Mikhail M. Ivanov[b,c†] and Sergey Sibiryakov[c,b‡]

[a] *Theory Group, Physics Department, CERN, CH-1211 Geneva 23, Switzerland*

[b] *Faculty of Physics, Moscow State University, Vorobjevy Gory, 119991 Moscow, Russia*

[c] *Institute for Nuclear Research of the Russian Academy of Sciences, 60th October Anniversary Prospect, 7a, 117312 Moscow, Russia*

Abstract

We study the possibility to constrain deviations from Lorentz invariance in dark matter (DM) with cosmological observations. Breaking of Lorentz invariance generically introduces new light gravitational degrees of freedom, which we represent through a dynamical timelike vector field. If DM does not obey Lorentz invariance, it couples to this vector field. We find that this coupling affects the inertial mass of small DM halos which no longer satisfy the equivalence principle. For large enough lumps of DM we identify a (chameleon) mechanism that restores the inertial mass to its standard value. As a consequence, the dynamics of gravitational clustering are modified. Two prominent effects are a scale dependent enhancement in the growth of large scale structure and a scale dependent bias between DM and baryon density perturbations. The comparison with the measured linear matter power spectrum in principle allows to bound the departure from Lorentz invariance of DM at the per cent level.

1 Introduction

Elucidating the nature of dark matter (DM) stands as a major challenge of modern cosmology and particle physics. One of the basic properties always assumed is that DM satisfies Lorentz invariance (LI). In this work we want to analyze how this assumption can be verified from the study of cosmological perturbations.

Lorentz invariance is one of the best tested symmetries of the Standard Model of particle physics [1]. Thus, it is tempting to postulate that it is a fundamental property of all fields of Nature including gravity and the dark sectors of the Universe, i.e DM and dark energy.

*diego.blas@cern.ch

†mm.ivanov@physics.msu.ru

‡sibir@inr.ac.ru; sergey.sibiryakov@cern.ch

This assumption is very powerful, but also restrictive. When applied to gravitation it has far-reaching conceptual implications, like the uniqueness of General Relativity (GR) as the LI theory of gravity, see e.g. [2, 3, 4, 5]. However, beautiful as it is, GR suffers from the problem of non-renormalizability precluding its interpretation as a UV complete quantum theory. This is the essence of the notorious problem of quantum gravity.

It is conceivable that the eventual theory of quantum gravity will involve violation of LI (Lorentz violation, LV, for short) in some form. For instance, it was recently suggested by P. Hořava that a UV completion of GR may be possible within perturbative quantum field theory at the cost of abandoning LI at very high energies [6]. This approach appears promising as it allows for an immediate improvement compared to GR coming from the softening of the gravitational amplitudes in the UV[1] [7]. If deviations from LI are present in quantum gravity, it is mandatory to understand which are the consequences for the rest of fields in Nature [8, 9].

A first relevant observation is that even when introduced at very high energies, LV has also consequences at low energies [10]. Indeed, LV corresponds to the existence of a preferred reference frame at every point of space-time. Additional local fields are required to set up this frame; those have typically massless excitations and affect physics at any scale. The situation at low-energies is encapsulated by the so-called Einstein-aether model [11, 12] where the preferred frame is determined by a vector field with unit norm (aether). This model is an effective theory with a cutoff that can be as high as the Planck mass [13]. Restricting the aether to its longitudinal component one obtains the khronometric model that was introduced in [14] as the low-energy limit of the Hořava's proposal we just mentioned [7, 15] (more precisely, of its healthy extended version [16]). In both Einstein-aether and khronometric cases, the interaction of the aether with the metric field has consequences for gravitation at all distances, which leads to observable astrophysical and cosmological effects [12, 17, 18].

Precision tests of LI in the Standard Model of particle physics put extremely tight constraints on the coupling of the aether to ordinary matter [1, 8]. If similar bounds held for the couplings of the aether to other sectors of the Universe, LV would have no effect on cosmology. In this paper we adopt the viewpoint that there is a mechanism that enforces LI of the Standard Model with the required precision while allowing for sizable LV in gravitational physics, DM or dark energy. Finding such mechanism while avoiding fine-tuning is an important challenge for the model and a few possibilities have been proposed in [19, 20, 21]. Some consequences of LV for dark energy were unveiled in [22], where it was shown that the presence of the aether vector field allows to attribute the current acceleration of the Universe to a renormalizable operator not sensitive to UV corrections. The present work is devoted to a systematic investigation of LV effects in the cosmological evolution of DM. To isolate these effects we will assume throughout the paper that the dark energy is represented by the cosmological constant.

We consider a general set-up, with DM described in terms of an effective fluid that interacts with the aether to account for LV. The simplest DM candidate described within

[1] One should keep in mind though that the renormalizability of gravity in the strict sense along these lines has not yet been demonstrated due to the complexity of the resulting theory.

our formalism is the theory of massive non-relativistic particles, but other possibilities, such as axionic DM [23], are also covered. We will assume that the velocities of DM are non-relativistic during the observable evolution of the Universe. One might think that this would suppress all LV effects. However, this is not the case. We will see that the coupling to the aether modifies the inertial mass of the DM particles, but does not affect their gravitational mass. As a consequence, DM violates the equivalence principle and the dynamics of cosmological perturbations change. The situation resembles that in LI theories with additional long-range interaction in the DM sector [24, 25]. However, the specific signatures of LV allow to distinguish between these two cases.

It is worth pointing out that a future direct detection of DM may yield strong constraints on LV in this sector. Indeed, a direct detection would imply a relatively strong coupling between the DM and visible sectors. In that case LV would be transferred from DM to ordinary matter via loop diagrams and thus would be subject to the tight existing bounds on LV in the Standard Model. Similar arguments were used in [26, 27] to constrain violation of the equivalence principle in the DM sector in the LI context. However, in the absence of any direct detection so far and since the loop calculations are rather model-dependent, we find it useful to study the bounds on LV in DM following from its gravitational manifestations, in particular in cosmology.

Our work is organized as follows. In Sec. 2 we briefly review the Einstein-aether and khronometric models. To understand the qualitative effects of LV in DM we study in Sec. 3 the dynamics of massive point particles coupled to the aether, concentrating on the Newtonian limit and Jeans instability. We next proceed to the systematic treatment of LV DM using the effective fluid description. Sec. 4 contains the description of the setup, analysis of the homogeneous cosmology and the equations for the linearized perturbations. Sec. 5 contains the analytic study of the perturbations in various regimes and the qualitative discussion of the observational signatures. The results of the numerical integration of the linearized equations in a simplified cosmological model are presented in Sec. 6. Section 7 contains the summary and discussion of our results. Some technical details of our numerical procedure are described in the Appendix.

2 Gravity with a preferred frame

To describe LV we assume that at every point of space-time there is a time-like vector u_μ that following Ref. [11] we will call "aether". The vector is constrained to have unit norm[2],

$$u_\mu u^\mu = 1 \ . \tag{1}$$

Thus it does not vanish anywhere and sets the preferred time-direction at every point of space-time. This breaks the local Lorentz group $SO(3,1)$ of GR to the local subgroup $SO(3)$

[2]We use the metric with $(+,-,-,-)$ signature. Latin indices from the middle of the alphabet take the values $i,j=1,2,3$, while Greek letters denote the space-time indices. The latter are manipulated with $g_{\mu\nu}$. Objects in bold face are three-vectors. We use units where the speed of propagation of light is $c=1$.

of purely spatial rotations that leave u_μ invariant. This way, the introduction of u_μ allows us to describe LV effects with an action invariant under arbitrary coordinate transformations. We will be interested in the dynamics of u_μ at large distances, which according to the rules of effective field theory is governed by operators with the smallest number of derivatives. It is straightforward to see that it is impossible to construct any contribution to the Lagrangian with one or no derivatives. Thus LV at low-energies is governed by the action of the Einstein-aether model [11, 12], the most general action containing up to two derivatives of u_μ,

$$S_{æ} \equiv -\frac{M_0^2}{2}\int \mathrm{d}^4x\sqrt{-g}\Big[R + K^{\mu\nu}{}_{\sigma\rho}\nabla_\mu u^\sigma \nabla_\nu u^\rho + l(u_\mu u^\mu - 1)\Big]\,, \tag{2}$$

where

$$K^{\mu\nu}{}_{\sigma\rho} \equiv c_1 g^{\mu\nu}g_{\sigma\rho} + c_2\delta^\mu_\sigma\delta^\nu_\rho + c_3\delta^\mu_\rho\delta^\nu_\sigma + c_4 u^\mu u^\nu g_{\sigma\rho}, \tag{3}$$

and the last term with the Lagrange multiplier l has been added to enforce the unit-norm constraint. We have included in the above action the Einstein-Hilbert term for the metric $g_{\mu\nu}$. The parameter M_0 is related to the Planck mass, cf. (9), while the dimensionless constants c_a, $a = 1, 2, 3, 4$, characterize the strength of the interaction of the aether with gravity. As discussed below, observations require these constants to be much less than 1, so we will assume

$$|c_a| \ll 1 \tag{4}$$

throughout the paper. Let us stress again that while we are interested in describing LV, the action (2) is explicitly generally covariant. This stems from the assumption that the non-vanishing aether field represents the only source of LV. In a certain sense, the picture is analogous to the spontaneous symmetry breaking of internal symmetries[3]. Finally, as an effective theory Einstein-aether has a cutoff of order $M_0|c_a|^{1/2}$ [13]. If c_a are not extremely small this cutoff is only a few orders of magnitude below the Planck mass.

A variant of the Einstein-aether model is obtained by restricting the aether to be hypersurface-orthogonal,

$$u_\mu \equiv \frac{\partial_\mu\sigma}{\sqrt{g^{\mu\nu}\partial_\mu\sigma\partial_\nu\sigma}}\,. \tag{5}$$

In this case the unit-norm constraint is identically satisfied and the Lagrange multiplier term in the action (2) can be omitted. The expression (5) is invariant under reparameterizations

$$\sigma \mapsto \tilde\sigma(\sigma)\,, \tag{6}$$

where $\tilde\sigma(\sigma)$ is an arbitrary monotonic function. The scalar field σ is assumed to have a time-like gradient at every point of space-time. This defines a preferred time-coordinate, hence

[3]There is an important difference though. The condition (1) excludes from consideration any LI states thus precluding the symmetry restoration. The attempt to make the length of u_μ dynamical to allow for the restored symmetry phase leads to appearance of a ghost degree of freedom that spoils the theory [28]. The absence of a healthy LI phase is common to gravitational models with LV, which raises doubts about the possibility to UV complete them within a LI setting, see the discussion of this issue in [29, 30].

σ is called "khronon" (from the Greek word for "time"), and the class of models including the metric and σ "khronometric" models. When restricted to the form (5), the curl of the aether vanishes

$$\omega^\mu \equiv \epsilon^{\mu\nu\lambda\rho} u_\nu \nabla_\lambda u_\rho = 0 \ . \tag{7}$$

As a consequence, the four combinations with derivatives of u_μ in the action (2) are not independent. It is common to eliminate the c_1-term in favor of the other three. The coefficients for the last three operators in (3) then become

$$\lambda \equiv c_2 \ , \quad \beta \equiv c_3 + c_1 \ , \quad \alpha \equiv c_4 + c_1 \ . \tag{8}$$

This model naturally arises as the low-energy limit of Hořava gravity [15, 14]. In other words, Hořava gravity can provide a UV completion for the khronometric theories which potentially improves their UV behavior as compared to GR.

The main difference between Einstein-aether and khronometric models is the number of degrees of freedom. Einstein-aether describes three types of massless propagating modes: the standard transverse-traceless tensor modes of the metric and the vector and scalar polarizations coming from the transverse and longitudinal fluctuations of the aether. For the khronometric case, the transverse vector polarization is absent. In the scalar and tensor sectors the two models are almost equivalent[4]. As in this paper we are mostly interested in the scalar cosmological perturbations, we will often use without loss of generality the terminology of the khronometric model and, in particular, the constants (8). One can show that the parameters c_a (or (8) for the khronometric case) can be chosen such that all modes are stable and have positive energy [12, 16]. To avoid gravitational and aether Cherenkov losses by high-energy cosmic rays [28], one should also require that the velocities of the graviton and aether modes are not less than the speed of high-energy particles comprising the cosmic rays, which is close to one.

The phenomenology of theories with action (2) has been extensively studied [12, 14, 18]. The high precision with which LI is tested within the Standard Model excludes the direct interaction of the aether with baryonic matter[5], meaning that the latter couples universally to the metric $g_{\mu\nu}$. Still, the aether affects the gravitational field of matter sources. At the Newtonian level the modifications amount to an unobservable renormalization of the gravitational constant that now reads [32, 16],

$$G_N \equiv \frac{1}{8\pi M_0^2}\left(1 - \frac{c_1 + c_4}{2}\right)^{-1} \ . \tag{9}$$

The deviations from GR for Solar System physics are encoded in two post-Newtonian parameters α_1^{PPN} and α_2^{PPN}. These have been calculated for the generic aether in Ref. [33] and for the khronometric model in Refs. [14, 18]. Observations yield the constraints [34]

$$|\alpha_1^{PPN}| \lesssim 10^{-4} \ , \qquad |\alpha_2^{PPN}| \lesssim 4 \cdot 10^{-7} \ . \tag{10}$$

[4] The only difference is the presence of an instantaneous mode in the khronometric model, which is absent in Einstein-aether [31]. This difference is not relevant for the local physics that we study in the present work.

[5] Examples of mechanisms to suppress such interaction are discussed in [19, 20, 21].

Those constraints are trivially satisfied in GR, where $\alpha_1^{PPN} = \alpha_2^{PPN} = 0$. For LV theories with generic parameters they imply the condition

$$|c_a| \lesssim 10^{-7} \,. \tag{11}$$

This bound is relaxed for certain relations between the parameters. In the generic aether model one can impose two restrictions on c_a to make both α_1^{PPN} and α_2^{PPN} vanish [12]. Then one is left with a two-parameter family of theories that are indistinguishable from GR at the post-Newtonian level (i.e. for Solar System tests [35]). Remarkably, for the khronometric case the same is achieved by the single condition $\alpha = 2\beta$, which leaves the parameters β and λ arbitrary. Further bounds of order

$$|c_a| \lesssim 10^{-2} \tag{12}$$

follow from considerations of Big Bang Nucleosynthesis (BBN) [32] and emission of gravitational waves by binary systems [36, 18].

To sum up, the theory (2) with universal coupling of ordinary matter to the metric $g_{\mu\nu}$ is phenomenologically viable provided the stability constraints are satisfied and (4) holds at the level of (11) or (12) (in the latter case the relations ensuring vanishing of the PPN parameters must be fulfilled).

3 Lorentz violating dark matter: point-particles

To grasp the physical consequences of LV in the DM sector we first study how the coupling to the aether affects the dynamics of gravitationally interacting point particles. This will allow us to understand the Newtonian limit of the theory and the effects of LV on the Jeans instability.

In the presence of the aether the relativistic action for a massive point particle can be generalized to

$$S_{pp} \equiv -m \int \mathrm{d}s \; F(u_\mu v^\mu) \,, \tag{13}$$

where

$$\mathrm{d}s \equiv \sqrt{g_{\mu\nu}\mathrm{d}x^\mu \mathrm{d}x^\nu} \tag{14}$$

is the proper length along the trajectory of the particle and

$$v^\mu \equiv \frac{\mathrm{d}x^\mu}{\mathrm{d}s} \tag{15}$$

is the particle's four-velocity. F is an arbitrary positive function that we normalize to $F(1) = 1$; the GR limit corresponds to $F \equiv 1$. Note that particles described by the action (13) violate the equivalence principle and, actually, do not follow geodesics of any metric.

It is instructive to work out the relation between the covariant description based on the action (13) and the approach commonly adopted in the study of LV in microphysics. In the latter approach LV manifests itself for free particles in the modified dispersion relation [37]

$$E^2 = \mathcal{E}^2(\mathbf{p}^2) \,, \tag{16}$$

where E and $\mathbf{p}$ are the energy and momentum of the particle in the preferred frame where the aether is aligned with the time direction, $u_0 = 1,\ u_i = 0$, and $\mathcal{E}^2$ is a function that takes the form,

$$\mathcal{E}^2 = m^2 + \mathbf{p}^2 \,,$$

if LI is preserved. The preferred frame singles out a preferred time coordinate t and through (13) defines the Lagrangian

$$S_{pp} = \int \mathrm{d}t\ L_{pp} \,, \tag{17}$$

where

$$L_{pp} = -m\sqrt{1-\mathbf{V}^2}\ F\!\left(\frac{1}{\sqrt{1-\mathbf{V}^2}}\right) , \qquad V^i \equiv \frac{\mathrm{d}x^i}{\mathrm{d}t} \,. \tag{18}$$

The energy and momentum are now related to the velocity V^i by the standard formulas

$$E = V^i\,\frac{\partial L_{pp}}{\partial V^i} - L_{pp}, \quad p_i = \frac{\partial L_{pp}}{\partial V^i} \,. \tag{19}$$

For a given function F these equations yield an implicit relation between E and p_i, i.e. the dispersion relation of the form (16). Vice versa, starting from the dispersion relation (16) one obtains the equation for the Lagrangian

$$\left(V^i\,\frac{\partial L_{pp}}{\partial V^i} - L_{pp}\right)^2 = \mathcal{E}^2\!\left(\frac{\partial L_{pp}}{\partial V^i}\frac{\partial L_{pp}}{\partial V^i}\right) . \tag{20}$$

We conclude that there is a one-to-one correspondence between the functions F of the covariant approach and the functions $\mathcal{E}^2$ appearing in the free-particle dispersion relation.

Let us solve Eq. (20) in the simplest case of the quadratic dispersion,

$$E^2 = m^2 + (1+\xi)\mathbf{p}^2 \,, \tag{21}$$

where ξ is a dimensionless constant. Under fairly general assumptions this type of dispersion relations with $\xi \neq 0$ describes the leading effect of LV at relatively low energies [38]. In this case we observe that by the redefinition $\tilde{V}^i \equiv V^i(1+\xi)^{-1/2}$ equation (20) reduces to the standard relativistic form. Thus we obtain,

$$L_{pp} = -m\sqrt{1-\tilde{\mathbf{V}}^2} = -m\sqrt{1-\frac{\mathbf{V}^2}{1+\xi}} \,, \tag{22}$$

and finally

$$S_{pp} = -m \int \mathrm{d}s \sqrt{\frac{1+\xi\,(u_\mu v^\mu)^2}{1+\xi}}\,. \tag{23}$$

As discussed above, this case encompasses a wide class of physically interesting situations. However, since imposing the specific form (23) does not simplify the analysis, and also to be completely general, we will continue to work with an arbitrary function F.

3.1 Newtonian limit

We will assume that DM is non-relativistic during the relevant stages of cosmological evolution, i.e. it moves slowly with respect to the cosmic frame. The latter is defined as the frame where the cosmic microwave background (CMB) is approximately isotropic. We will assume that it coincides with the preferred frame set by the background value of the aether[6]. Thus one can use the Newtonian limit to describe the dynamics at subhorizon scales. This corresponds to expanding the action (13) to quadratic order in the particle three-velocities V^i, quadratic order in the spatial component of the aether[7] u^i and to linear order in the Newton potential ϕ. The latter appears in the standard Newtonian limit of the metric[8],

$$g_{00} = 1 + 2\phi\ , \quad g_{0i} = 0\ , \quad g_{ij} = -\delta_{ij}(1-2\psi)\ , \tag{24}$$

where for the moment we have neglected the cosmological expansion. We obtain

$$S_{pp} = m \int \mathrm{d}t \left[\frac{(V^i)^2}{2} - \phi - Y\frac{(u^i - V^i)^2}{2}\right], \tag{25}$$

where we have denoted

$$Y \equiv F'(1) \tag{26}$$

and omitted the constant term corresponding to the rest-mass. To understand the effect of LV, we consider first the case when the aether fluctuations are negligible, $u^i = 0$. In this case the last term in (25) renormalizes the particle's inertial mass

$$m \mapsto m(1-Y)\ .$$

On the other hand, the gravitational mass (the source of ϕ in (25)) remains equal to m, which clearly violates the equivalence principle. To guarantee the positivity of the kinetic energy we impose the restrictions $m > 0$ and $Y < 1$.

[6]This is justified since it has been shown [39] that in a homogeneous expanding universe the aether field tends to align with the time direction.

[7]We assume that u^i is of the same order as V^i, as will be verified by the calculation for the self-gravitating situation given below. The presence of the direct coupling between DM particles and the aether is crucial for that. In the absence of such coupling, as it happens for the field produced by visible matter [33, 18], the aether has the order $O(V^3)$ and the dynamics of the system is different.

[8] Other metric perturbations are of higher post-Newtonian order.

Let us now consider the generic situation in the Newtonian limit for a dense medium composed of DM particles. It is convenient to introduce the mass density,

$$\rho(\mathbf{x},t) = m\sum_A \delta^{(3)}(\mathbf{x}-\mathbf{x}_A(t)) \,, \tag{27}$$

where $\mathbf{x}_A(t)$ is the trajectory of the A-th particle, and rewrite the action (25) in the form,

$$S_{pp} = \int \mathrm{d}^4x\, \rho \left[\frac{(V^i)^2}{2} - \phi - Y\frac{(u^i-V^i)^2}{2}\right] . \tag{28}$$

One observes that inside the medium the aether perturbations acquire a quadratic potential with the central value set by the velocity of the medium. Not to destabilize the aether the potential must be positive[9], $Y > 0$. We can anticipate that due to this potential the aether tends to align with the velocity of the medium. When alignment occurs, the last term in (28) disappears, restoring the standard action for the fluid universally coupled to gravity. In other words, the violation of equivalence principle will be screened inside a dense medium, realizing an analog of the chameleon mechanism [40]. This picture is elaborated quantitatively in what follows.

The action (28) must be supplemented by the non-relativistic limit of the Einstein-aether action (2). For simplicity, in the rest of this section we will restrict to the case $c_2 = c_3 = c_4 = 0$ and describe the results to leading order in $c_1 \ll 1$. This limit shows already the key features of the generic case, to be considered in Sec. 4.4. In this approximation, the action (2) at post-Newtonian order reads

$$S_{æ} = \frac{M_0^2}{2}\int \mathrm{d}^4x \big[4\phi\Delta\psi - 2\psi\Delta\psi + c_1 u^i\Delta u^i\big] \,. \tag{29}$$

Additionally, we will assume $c_1 \lesssim Y$. This is the most interesting regime from the phenomenological perspective since we do not expect to obtain bounds on the LV in DM matter sector that would be much stronger than the bounds on c_1.

The equations of motion following from (28) and (29) are[10]

$$(1-Y)\,\dot V^i + \partial_i\phi + Y(\partial_t u^i + V^j\partial_j u^i - V^j\partial_i u^j + u^j\partial_i u^j) = 0 \,, \tag{30a}$$

$$\psi = \phi \,, \tag{30b}$$

$$2M_0^2\Delta\phi = \rho \,, \tag{30c}$$

$$M_0^2 c_1\Delta u^i = Y\rho\,(u^i - V^i) \,. \tag{30d}$$

This system is closed by adding the continuity equation for DM,

$$\partial_t\rho + \partial_i(\rho V^i) = 0 \,. \tag{30e}$$

[9]The case of negative Y can also be interesting from the phenomenological viewpoint if the growth of the instability induced by the negative potential is smaller or comparable to the Hubble rate. To satisfy this requirement the absolute value of Y must be of order c_a, cf. Eq. (31), which already sets a strong restriction on LV in DM.

[10]In this and only in this section dot denotes the total (material) derivative with respect to t.

Consider a spherical DM halo of size R_h, constant density ρ_h and moving as a whole with velocity $\mathbf{V}_h$ with respect to the preferred frame. According to Eq. (30d) the aether perturbations inside the halo acquire the effective mass

$$m_{\rm eff}^2 = \frac{Y\rho}{M_0^2 c_1} \ . \tag{31}$$

Let us first assume that the halo is small,

$$R_h \ll m_{\rm eff}^{-1} \ , \tag{32}$$

so that the range of the aether interactions exceeds the halo size. Note that this condition is equivalent to

$$\phi_{h,s} \ll c_1/Y \ , \tag{33}$$

where $\phi_{h,s} \sim \rho_h R_h^2/M_0^2$ is the gravitational potential at the surface of the halo. Then in (30d) one can neglect the u^i-term on the r.h.s. and obtain for the aether field produced by the halo,

$$u^i = -\frac{2YV_h^i}{c_1}\,\phi_h(\mathbf{x},t) \ , \tag{34}$$

where we have expressed the result in terms of the halo's gravitational potential

$$\phi_h(\mathbf{x},t) = -\frac{\rho_h R_h^3}{6M_0^2|\mathbf{x}-\mathbf{V}_h t|} \ . \tag{35}$$

We now study the motion of a test DM particle in the field of the halo. Substituting (34) into (30a) we obtain for the particle's acceleration

$$\dot V_{tp}^i = -\frac{\partial_i\phi_h}{1-Y} + \frac{2Y^2}{(1-Y)c_1}\big[-V_{tp}^jV_h^j\partial_i\phi_h + V_h^iV_{tp}^j\partial_j\phi_h - V_h^iV_h^j\partial_j\phi_h\big] \ . \tag{36}$$

One observes two modifications compared to the standard case. First, the gravitational acceleration towards the halo is enhanced by the factor $1/(1-Y)$ due to the reduction of the inertial mass of the test particle. This effect will play a key role in what follows. Second, the combination in the square brackets gives rise to the velocity-dependent interaction[11] discussed in [14]. The latter interaction is important as compared to the change in the gravitational acceleration only if the halo and the particle move fast enough,

$$|\mathbf{V}_{h,tp}| \gtrsim \sqrt{\frac{c_1}{Y}} \ . \tag{37}$$

[11]Note that this interaction violates the (naive) third Newton's law: e.g. for a two-body system $m_{(1)}\dot V_{(1)}^i + m_{(2)}\dot V_{(2)}^i \neq 0$. This is consistent with the observation [14] that in the presence of velocity dependent forces the conserved momentum contains additional contributions, depending both on the velocities and the distance between the bodies (see also [35]).

We are going to see (cf. (52)) that the bulk velocities of the linearized cosmological perturbations never satisfy the condition (37), so that the velocity-dependent forces do not play a significant role in the evolution of the Large Scale Structure. However, they may influence the dynamics of non-linear structures such as galaxies and galaxy clusters. We leave the study of this issue for the future.

Now consider the case when the size of the halo is larger than the inverse of the aether mass in its interior,

$$R_h \gg m_{\rm eff}^{-1} \ . \tag{38}$$

Equivalently,

$$\phi_{h,s} \gg c_1/Y \ . \tag{39}$$

Due to the Yukawa screening, the aether field is frozen at the minimum of its potential, $u^i = V_h^i$ over most of the halo volume, deviating from this value only in a surface layer of width $m_{\rm eff}^{-1}$. Neglecting this deviation, to leading order the aether field outside the halo is

$$u^i = \frac{R_h V_h^i}{|\mathbf{x} - \mathbf{V}_h t|} \ . \tag{40}$$

Clearly, this is smaller than (34) provided (39) holds. Thus the velocity-dependent interaction of a test particle with the halo is suppressed in this case. One notices the similarity with the chameleon mechanism [40] that screens scalar interaction in certain scalar-tensor gravity models. However, it should be stressed that the motion of a test particle is still modified compared to GR due to the renormalization of the gravitational acceleration (cf. (36)).

Finally, instead of the test particle one can consider another large halo, such that its own gravitational potential satisfies (39). Let us denote its velocity by $\mathbf{V}_{h1}$. Irrespectively of the aether configuration outside, in the interior of this halo the aether will coincide with V_{h1}^i. Substituting this into (30a) we obtain the standard equation,

$$\dot{V}_{h1}^i = -\partial_i \phi_h \ . \tag{41}$$

One concludes that for large halos the deviations from GR are completely screened[12].

3.2 Jeans instability

In this subsection we analyze how the above peculiarities of DM dynamics in the presence of LV affect the development of the Jeans instability. For simplicity, we will consider the universe filled exclusively with DM; the more realistic case including the cosmological constant, baryons and radiation will be studied in subsequent sections. Following the standard treatment of the Jeans instability in the Newtonian limit, we take the spherically symmetric

[12]One may wonder if this screening mechanism can work for ordinary matter and help to relax some constraints on LV in the Standard Model. Unfortunately this is not the case as in the Standard Model LI is tested for individual elementary particles.

Ansatz for the background values of the fields which we denote with an over-bar. In this case the solution to Eqs. (30) reads

$$\bar{V}^i = \bar{u}^i = H(t)\, x^i \ , \qquad \bar{\phi} = \frac{\bar{\rho}(t)}{12M_0^2}|\mathbf{x}|^2 \ , \tag{42}$$

where the Hubble parameter H and the density $\bar{\rho}$ are related by

$$\dot{H} + H^2 = -\frac{\bar{\rho}}{6M_0^2} \ , \tag{43a}$$

$$\dot{\bar{\rho}} + 3H\bar{\rho} = 0 \ . \tag{43b}$$

These are the standard equations of GR. In particular, introducing the scale factor

$$a(t) = \exp\left[\int^t H(t')\mathrm{d}t'\right] \tag{44}$$

and integrating Eqs. (43) once, we obtain the Friedmann equation

$$H^2 = \frac{\bar{\rho}}{3M_0^2} + \frac{\kappa}{a^2}, \tag{45}$$

with $\bar{\rho} \propto a^{-3}$. Thus at the level of the homogeneous cosmology the model reproduces[13] GR. In what follows we will set the spatial curvature to zero, $\kappa = 0$.

The next step is to write down the equations for the linear perturbations. We obtain

$$(1-Y)(\partial_t V^i + Hx^j\partial_j V^i + HV^i) + \partial_i\phi + Y(\partial_t u^i + Hx^j\partial_j u^i + Hu^i) = 0 \ , \tag{46a}$$

$$2M_0^2\Delta\phi = \bar{\rho}\,\delta \ , \tag{46b}$$

$$M_0^2 c_1 \Delta u^i = Y\bar{\rho}\,(-V^i + u^i) \ , \tag{46c}$$

$$\partial_t\delta + Hx^i\partial_i\delta + \partial_i V^i = 0 \ , \tag{46d}$$

where for simplicity we denote the perturbations by the same letters as the total quantities. We have introduced the density contrast $\delta = \delta\rho/\bar{\rho}$. Performing the Fourier decomposition

$$\delta \mapsto \mathrm{e}^{i\mathbf{k}\mathbf{x}/a(t)}\delta \ , \ \text{etc.} \ , \tag{47}$$

restricting to the longitudinal part

$$V^i = ik_i v \ , \qquad u^i = ik_i u \ , \tag{48}$$

and solving (46b), (46d) for ϕ and v we are left with two equations

$$(1-Y)(\partial_t^2\delta + 2H\partial_t\delta) - \frac{3H^2}{2}\,\delta + Y\frac{k^2}{a}(\partial_t u + Hu) = 0 \ , \tag{49a}$$

$$\left[c_1 M_0^2\frac{k^2}{a^2} + Y\bar{\rho}\right] u = \frac{Y\bar{\rho}\,a}{k^2}\,\partial_t\delta \ . \tag{49b}$$

[13] As will be discussed in Sec. 4, there is actually a mismatch between the gravitational constant appearing in the Friedmann equation and the locally measured value (cf. (87)). This mismatch is of order c_a and is not captured by the approximation used in this section.

Here we have used the Friedmann equation (45) to express the factor in the second term of (49a) through the Hubble parameter.

The form of Eq. (49b) suggests to distinguish two regimes. For short waves,

$$\frac{k^2}{a^2} \gg \frac{Y\bar{\rho}}{M_0^2 c_1} \,, \tag{50}$$

the aether perturbation reads

$$u = \frac{Y\bar{\rho}\, a^3}{M_0^2 c_1 k^4} \partial_t \delta \,. \tag{51}$$

Note that the inequality (50) is nothing but the condition for the unscreened regime, Eq. (32), with the size of the halo replaced by the physical wavelength a/k of the perturbation. Upon substitution into (49a) the aether gives only a small correction that can be neglected. This can be understood as neglecting the velocity-dependent interaction. Indeed, one estimates the velocity perturbation as (see (46d)),

$$|\mathbf{V}| \sim H\delta \frac{a}{k} \ll H\delta \sqrt{\frac{M_0^2 c_1}{Y\bar{\rho}}} \sim \delta \sqrt{\frac{c_1}{Y}} \ll \sqrt{\frac{c_1}{Y}}, \tag{52}$$

where in the third relation we used the background Friedmann equation; this is below the limit (37). Thus for the density contrast we obtain the equation,

$$\partial_t^2 \delta + 2H\partial_t \delta - \frac{3H^2}{2(1-Y)}\,\delta = 0 \,. \tag{53}$$

Its growing solution has the form

$$\delta \propto t^\gamma \,, \qquad \gamma = \frac{1}{6}\left[-1 + \sqrt{\frac{25-Y}{1-Y}} \right] , \tag{54}$$

Clearly, for $Y > 0$ the mode grows faster than in GR where $\gamma = 2/3$.

In the opposite regime of long modes,

$$\frac{k^2}{a^2} \ll \frac{Y\bar{\rho}}{M_0^2 c_1} \,, \tag{55}$$

the aether takes the form

$$u = \frac{a}{k^2}\, \partial_t \delta \,. \tag{56}$$

The corresponding contribution in (49a) combines with the first term and restores the standard equation for the density perturbations in GR as expected in the screened regime,

$$\partial_t^2 \delta + 2H\partial_t \delta - \frac{3H^2}{2}\,\delta = 0 \,, \tag{57}$$

whose solution is $\delta \propto t^{2/3}$.

The following picture emerges from the above results. For a mode with given k the effects of LV are screened as long as the inequality (55) is satisfied and the mode behaves exactly as in GR. As the universe expands, this inequality breaks down[14] and the mode enters into the unscreened regime, where its growth is accelerated up to (54). Physically, this enhancement is due to the increase in the gravitational acceleration of the DM particles in this regime, see Eq. (36), which in turn is due to the change in their inertial mass. We will see in Sec. 5 that this picture coincides with the results of the full relativistic analysis in the appropriate limit (subhorizon modes, matter dominated epoch).

Before closing this section, we mention that a straightforward analysis of the transverse (vector) modes of the perturbations shows that these modes decay in the same way as in GR both in the long- and short-wave regimes. We will not consider the vector modes in what follows.

4 Lorentz violating dark matter: relativistic fluid

To systematically develop the consequences of the aether – DM interaction beyond the Newtonian limit it is convenient to use a relativistic fluid description of DM. The most suitable for our purposes is the pull-back formalism, which enables to describe perfect fluids with arbitrary equation of state using an effective action, see [41] for a review and early references. Since the reader may not be familiar with this formalism, we give a succinct review of it in the next subsection, closely following the presentation of [29]. We will specialize in the case of cold DM with vanishing pressure and present an effective action describing its interaction with the aether. In Sec. 4.2 we use this action to derive the equations of motion. Then in Secs. 4.3, 4.4 we analyze the consequences of the resulting model for the background cosmology and derive the equations for linear perturbations around Friedmann–Lemaître–Robertson–Walker (FLRW) solutions.

4.1 Effective action for Lorentz violating fluids

In the pull-back formalism, the fluid elements are labeled by three scalar fields $\varphi^I(x)$, $I = 1, 2, 3$. An essential property of a perfect fluid is the invariance of its dynamics when its elements are moved around without changing their volume. This means that the description in terms of the fields $\varphi^I(x)$ must be invariant under volume-preserving reparameterizations

$$\varphi^I \mapsto \tilde{\varphi}^I(\varphi^J) \,, \qquad \det \frac{\partial \tilde{\varphi}^I}{\partial \varphi^J} = 1 \,. \tag{58}$$

The scalar object with the minimal number of derivatives invariant under (58) that can be constructed from φ^I and the metric $g_{\mu\nu}$ is

$$B \equiv -\det B^{IJ} \,, \tag{59}$$

[14] Recall that $\bar{\rho}$ decays as a^{-3} so that the r.h.s. of (55) decreases faster than the l.h.s.

where

$$B^{IJ} = g^{\mu\nu}\partial_\mu\varphi^I\partial_\nu\varphi^J \ . \tag{60}$$

The Lagrangian for the perfect fluid is thus an arbitrary function of this quantity,

$$S_{fluid} = -\int \mathrm{d}^4x\sqrt{-g}\, f(B) \ . \tag{61}$$

To make contact with the standard quantities of hydrodynamics let us consider the vector[15]

$$v^\mu \equiv -\frac{\epsilon^{\mu\nu\sigma\rho}}{6\sqrt{-gB}}\,\partial_\nu\varphi^I\partial_\sigma\varphi^J\partial_\rho\varphi^K\epsilon_{IJK} \ . \tag{62}$$

This vector has unit norm, is future directed and has the property that the fluid labels φ^I remain constant along its integral curves

$$v^\mu\partial_\mu\varphi^I = 0, \qquad I = 1,2,3. \tag{63}$$

Thus it is identified with the fluid velocity. It follows that independently of the equations of motion

$$\nabla_\mu(\sqrt{B}\, v^\mu) = 0 \ , \tag{64}$$

which implies that $\sqrt{B}$ should be interpreted as the conserved number density n of the fluid elements. Other useful relations are

$$B_{IJ}\partial_\mu\varphi^I\partial_\nu\varphi^J = g_{\mu\nu} - v_\mu v_\nu \ , \qquad \partial_\nu\varphi^I\partial_\rho\varphi^J\partial_\sigma\varphi^K\epsilon_{IJK} = -\sqrt{-g\,B}\, v^\mu\epsilon_{\mu\nu\rho\sigma} \ , \tag{65}$$

where B_{IJ} is the inverse matrix of B^{IJ}. The energy-momentum tensor (EMT) following from (61) can be cast into the standard hydrodynamic form

$$T_{\mu\nu} = (\rho + p)v_\mu v_\nu - p g_{\mu\nu} \ ,$$

where the density and pressure are given by

$$\rho = f \ , \quad p = 2f'B - f \ . \tag{66}$$

It is conserved due to the equations of motion for the fields φ^I,

$$\nabla_\mu\big(f'(B)BB_{IJ}\nabla^\mu\varphi^J\big) = 0 \ . \tag{67}$$

For cold DM $p = 0$ implying that f takes the form,

$$f_{dm} = m\sqrt{B} = m\, n \ , \tag{68}$$

where m is the mass of the fluid elements.

[15]The antisymmetric pseudotensors are defined as $\epsilon^{0123} = -\epsilon_{0123} = -1$, $\epsilon_{123} = 1$.

It is clear how to generalize the action (61) to include the effects of LV. In the presence of the aether the action can also depend on the invariant scalar product $u_\mu v^\mu$,

$$\tilde{S}_{fluid} = -\int \mathrm{d}^4x\sqrt{-g}\,\tilde{f}(B, u_\mu v^\mu)\ . \tag{69}$$

Once the microscopic theory of DM is specified the function $\tilde{f}$ can in principle be computed. In this work we adopt a phenomenological approach and consider a generic function satisfying reasonable conditions. A natural assumption for DM is that the Lagrangian is proportional to the particle number,

$$\tilde{f}_{dm}(B, u_\mu v^\mu) = m\sqrt{B}\,F(u_\mu v^\mu)\ , \tag{70}$$

where the function F is subject to the normalization condition $F(1) = 1$. It is easy to convince oneself that most cold DM scenarios are described by functions of the form (70). In particular, this assumption is valid for DM composed of well-separated particles that weakly interact with each other. The function F then coincides with that appearing in the one-particle action considered in Sec. 3.

4.2 Equations of motion

The equations of motion for the DM fluid are obtained by varying (69) with respect to φ^I and read

$$\nabla_\mu\left[\sqrt{B}B_{IJ}\nabla^\mu\varphi^J\big(F - (u_\lambda v^\lambda)F'\big) + F'\frac{\epsilon^{\mu\nu\lambda\rho}}{2\sqrt{-g}}u_\nu\partial_\lambda\varphi^J\partial_\rho\varphi^K\epsilon_{IJK}\right] = 0\ . \tag{71}$$

A more conventional form involving only hydrodynamic variables emerges after contracting with $\partial_\sigma\varphi^I$ and using Eqs. (65),

$$-\nabla_\mu\Big[\rho_{[dm]}\Big(\big(F - (u_\lambda v^\lambda)F'\big)v^\mu v_\sigma + F'v^\mu u_\sigma\Big)\Big] + \rho_{[dm]}F'v^\mu\nabla_\sigma u_\mu = 0\ , \tag{72}$$

where we introduced

$$\rho_{[dm]} \equiv m\sqrt{B}\ . \tag{73}$$

The equations of motion for the aether are slightly different depending on whether one considers a generic aether or a khronon for the LV sector. In the former case, from the variation of the combination of (2) and (69) one finds

$$\nabla_\mu K^\mu{}_\nu - c_4 a^\rho\nabla_\nu u_\rho - l u_\nu - \frac{\rho_{[dm]}}{M_0^2}F'v_\nu = 0\ , \tag{74}$$

where we made use of the following notations,

$$K^\mu{}_\sigma \equiv K^{\mu\nu}{}_{\sigma\rho}\nabla_\nu u^\rho\ , \qquad a_\mu \equiv u^\lambda\nabla_\lambda u_\mu\,. \tag{75}$$

Contracting (74) with u^ν and using the constraint (1) we obtain the expression for the Lagrange multiplier,

$$l = u^\nu \nabla_\mu K^\mu{}_\nu - c_4 a^\rho a_\rho - \frac{\rho_{[dm]}}{M_0^2}(u_\mu v^\mu)F' \ . \tag{76}$$

When substituted back into (74), this yields,

$$\mathcal{P}^{\rho\mu}\left(\nabla_\nu K^\nu{}_\mu - c_4\, a_\nu \nabla_\mu u^\nu - \frac{\rho_{[dm]}}{M_0^2}F' v_\mu\right) = 0 \ , \tag{77}$$

where

$$\mathcal{P}^\nu_\mu \equiv \delta^\nu_\mu - u_\mu u^\nu \tag{78}$$

is the projector on the directions orthogonal to u_μ. In the khronon case the constraint is identically satisfied and thus the Lagrange multiplier is absent. Varying with respect to σ, we find the equation of motion which is essentially the divergence of (77),

$$\nabla_\rho\left[\frac{\mathcal{P}^{\rho\mu}}{\sqrt{\nabla^\lambda\sigma\nabla_\lambda\sigma}}\left(\nabla_\nu K^\nu{}_\mu - \alpha\, a_\nu \nabla_\mu u^\nu - \frac{\rho_{[dm]}}{M_0^2}F' v_\mu\right)\right] = 0 \ . \tag{79}$$

The EMT of DM is obtained by varying (69) with respect to the metric. In the case of the Einstein-aether we obtain

$$T_{[dm]\,\mu\nu} = \rho_{[dm]}\big(F - (u_\lambda v^\lambda)F'\big)v_\mu v_\nu \ . \tag{80}$$

In the khronometric model there is an extra contribution coming from the variation of u_μ when the metric is varied,

$$\tilde{T}_{[dm]\,\mu\nu} = \rho_{[dm]}\Big[\big(F - (u_\lambda v^\lambda)F'\big)v_\mu v_\nu + (u_\lambda v^\lambda)F' u_\mu u_\nu\Big] \ . \tag{81}$$

The difference between the previous expressions disappears once we consider the total EMT of the aether / khronon — DM system. This reads in both cases[16],

$$\begin{aligned} T_{[\mathrm{ae}]\,\mu\nu} + T_{[dm]\,\mu\nu} = M_0^2\Big[&2\nabla_\sigma K^\sigma{}_{(\mu}u_{\nu)} - \nabla_\lambda(K_{(\mu\nu)}u^\lambda) - \nabla_\sigma(K^\sigma{}_{(\mu}u_{\nu)}) + \nabla_\sigma(K_{(\mu}{}^\sigma u_{\nu)}) \\ &- c_1\nabla_\mu u^\lambda\nabla_\nu u_\lambda + c_1\nabla_\lambda u_\mu\nabla^\lambda u_\nu - 2c_4 u_{(\nu}\nabla_{\mu)}u^\sigma a_\sigma + c_4 a_\mu a_\nu \\ &+ \frac{1}{2}g_{\mu\nu}K^\sigma{}_\lambda\nabla_\sigma u^\lambda - u_\mu u_\nu u^\lambda\nabla_\sigma K^\sigma{}_\lambda + c_4 a_\rho a^\rho u_\mu u_\nu\Big] \\ &+ \rho_{[dm]}\Big(\big(F - (u_\lambda v^\lambda)F'\big)v_\mu v_\nu + (u_\lambda v^\lambda)F' u_\mu u_\nu\Big) \ , \end{aligned} \tag{82}$$

where in the aether case we have substituted the Lagrange multiplier from (76). The first three lines in (82) correspond to the pure aether EMT, while the last line represents the

[16]The indices in round brackets are symmetrized as $K_{(\mu\nu)} \equiv \frac{1}{2}(K_{\mu\nu} + K_{\nu\mu})$, etc.

contribution of DM and DM — aether interaction. Note that LV leads to the departure of the latter contribution from the perfect fluid form.

For the rest of the Universe we will consider the standard scenario with baryons, radiation and a cosmological constant[17]. Those possess EMT's,

$$T_{[b]\,\mu\nu} = \rho_{[b]} v_{[b]\,\mu} v_{[b]\,\nu} \ , \quad T_{[\gamma]\,\mu\nu} = \rho_{[\gamma]} \left(\frac{4}{3} v_{[\gamma]\,\mu} v_{[\gamma]\,\nu} - \frac{g_{\mu\nu}}{3} \right) \ , \quad T_{[\Lambda]\,\mu\nu} = \rho_{[\Lambda]} g_{\mu\nu} \ , \tag{83}$$

where $\rho_{[s]}$, $v_{[s]\,\mu}$ is the density and 4-velocity of the corresponding component. The equations of motion for these components are given by the covariant conservation of the EMT's (83). We neglect the energy exchange between baryons and radiation, as well as the effects due to neutrinos.

4.3 Background cosmology

The spatially homogeneous and isotropic Ansatz reads

$$\mathrm{d}s^2 = a^2(\tau)(\mathrm{d}\tau^2 - \mathrm{d}\mathbf{x}^2) \ , \quad u_0 = v_{[s]\,0} = a(\tau) \ , \quad u_i = v_{[s]\,i} = 0 \ , \quad \rho_{[s]} = \rho_{[s]}(\tau) \ , \tag{84}$$

where we have introduced the conformal time τ. It is straightforward to check that with this Ansatz Eq. (77) for the aether, or alternatively Eq. (79) for the khronon[18], is identically satisfied. Substituting (84) into (72) we find

$$\rho_{[dm]} \propto a^{-3} \ , \tag{85}$$

so the DM density behaves in the same way as in the standard FLRW universe. Using (82) we obtain the Friedmann equation,

$$\frac{\dot{a}^2}{a^4} = \frac{8\pi G_{cosm}}{3} \left(\rho_{[dm]} + \rho_{[b]} + \rho_{[\gamma]} + \rho_{[\Lambda]} \right) \ , \tag{86}$$

where dot denotes henceforth differentiation with respect to the conformal time. This has the same form as in GR, with the gravitational constant renormalized due to the contribution of the aether (khronon) EMT in the Einstein's equations (cf. [32]),

$$G_{cosm} = \frac{1}{8\pi M_0^2} \left[1 + \frac{\beta + 3\lambda}{2} \right]^{-1} \ . \tag{87}$$

Note that G_{cosm} differs from the Newton constant (9) measured in local experiments. This difference is constrained by the BBN considerations [32]

$$|G_{cosm}/G_N - 1| \lesssim 0.1 \ , \tag{88}$$

which places a rather mild bound on the aether parameters.

[17] As we want to isolate the effect of LV in the DM sector, we will not consider other possibilities for dark energy.

[18] The khronon field itself can be taken as an arbitrary monotonic function of time, e.g. $\sigma = \tau$.

4.4 Linear perturbations around FLRW

We now turn to the analysis of the linearized cosmological perturbations. We focus on scalar perturbations[19] and choose to work in the conformal Newtonian gauge,

$$\mathrm{d}s^2 = a(\tau)^2 \left[(1+2\phi)\mathrm{d}\tau^2 - \delta_{ij}(1-2\psi)\mathrm{d}x^i\mathrm{d}x^j\right] . \tag{89}$$

Since the scalar sectors of the Einstein-aether and khronometric theories are equivalent at the level of perturbations, it is enough to study the khronometric case with the parameters (8). For the perturbations of the aether vector, the velocities of various components and their densities we write

$$u_i = a\,\partial_i\chi\ , \quad v_{[s]\,i} = a\,\partial_i v_{[s]}\ , \quad u_0 = v_{[s]\,0} = a\,(1+\phi)\ , \quad \rho_{[s]} = \bar{\rho}_{[s]} + \delta\rho_{[s]}\ , \tag{90}$$

where $[s] = \{[dm],[b],[\gamma]\}$ and the overbar denotes the background values. Substituting these expansions into (82) and (83) we obtain the set of linearized Einstein's equations[20],

$$2\Delta\psi - 3\mathcal{H}(2+\alpha\mathcal{B})\dot{\psi} - \alpha\Delta\phi + \alpha\Delta\dot{\chi} + \alpha\mathcal{H}(1-\mathcal{B})\Delta\chi \\ - \frac{a^2}{M_0^2}(\delta\rho_{[dm]} + \delta\rho_{[b]} + \delta\rho_{[\gamma]} + 2\phi[\bar{\rho}_{[dm]} + \bar{\rho}_{[b]} + \bar{\rho}_{[\gamma]} + \rho_{[\Lambda]}) = 0\ , \tag{91a}$$

$$\dot{\psi} + \mathcal{H}\phi + \frac{\alpha\,\mathcal{C}^2\Delta\chi}{2+\alpha\mathcal{B}} - \frac{a^2}{M_0^2(2+\alpha\mathcal{B})}\left[\bar{\rho}_{[dm]}(Y\chi + (1-Y)v_{[dm]}) + \bar{\rho}_{[b]}v_{[b]} + \frac{4}{3}\bar{\rho}_{[\gamma]}v_{[\gamma]}\right] = 0\ , \tag{91b}$$

$$\ddot{\psi} + \mathcal{H}(\dot{\phi} + 2\dot{\psi}) + (2\dot{\mathcal{H}} + \mathcal{H}^2)\phi + \frac{2\Delta(\phi-\psi) + \alpha\mathcal{B}\Delta(\dot{\chi} + 2\mathcal{H}\chi)}{3(2+\alpha\mathcal{B})} - \frac{a^2\delta\rho_{[\gamma]}}{3(2+\alpha\mathcal{B})M_0^2} = 0\ , \tag{91c}$$

$$\phi - \psi - \beta(\dot{\chi} + 2\mathcal{H}\chi) = 0\ , \tag{91d}$$

where we defined

$$\mathcal{B} \equiv \frac{\beta+3\lambda}{\alpha}, \quad \mathcal{C}^2 \equiv \frac{\beta+\lambda}{\alpha}\,, \quad \mathcal{H} \equiv \frac{\dot{a}}{a}\,, \quad Y \equiv F'(1)\,. \tag{92}$$

[19] As we mentioned in Sec. 3.2, the vector perturbations decay as usual inside the horizon, so we do not expect any significant effect due to them. For the analysis of effects at cosmological distances in the Einstein-aether model with Lorentz invariant DM see [42]. Tensor modes behave as in GR with a modified speed of propagation [12, 18].

[20] In these and all subsequent equations dot denotes *partial* derivative with respect to τ.

We will assume in what follows that the parameters $\mathcal{B}$ and $\mathcal{C}$ are both of order one. The linearized khronon and DM equations are

$$\ddot{\chi} + 2\mathcal{H}\dot{\chi} - \mathcal{C}^2\Delta\chi + \left[\dot{\mathcal{H}}(1-\mathcal{B}) + \mathcal{H}^2(1+\mathcal{B}) + \frac{Y\bar{\rho}_{[dm]}a^2}{\alpha M_0^2}\right]\chi - \frac{Y\bar{\rho}_{[dm]}a^2}{\alpha M_0^2}v_{[dm]} - \dot{\phi} - \mathcal{H}(1+\mathcal{B})\phi - \mathcal{B}\dot{\psi} = 0 \,, \tag{93a}$$

$$\delta\dot{\rho}_{[dm]} + 3\mathcal{H}\delta\rho_{[dm]} - \bar{\rho}_{[dm]}(\Delta v_{[dm]} + 3\dot{\psi}) = 0 \,, \tag{93b}$$

$$\dot{v}_{[dm]} + \mathcal{H}v_{[dm]} + \frac{Y}{1-Y}(\dot{\chi} + \mathcal{H}\chi) - \frac{\phi}{1-Y} = 0 \,. \tag{93c}$$

From (93a) we see that the parameter $\mathcal{C}$ has the physical meaning of the velocity of the khronon waves. In what follows we will often use the integrated form of the last equation,

$$v_{[dm]} = -\frac{Y}{1-Y}\,\chi + \frac{1}{a(\tau)(1-Y)}\int^{\tau} \mathrm{d}\tau'\, a(\tau')\,\phi(\tau', \mathbf{x}) \,. \tag{94}$$

If the gravitational potentials are known, this can be used to eliminate $v_{[dm]}$ from (93a) and obtain an equation for χ. We observe that, as in the Newtonian limit, LV in DM is governed at the linear level by the single parameter Y. Following the discussion in Sec. 3, we will assume it to lie in the range $0 \leq Y < 1$.

For baryons and radiation we have the standard hydrodynamic equations,

$$\delta\dot{\rho}_{[b]} + 3\mathcal{H}\delta\rho_{[b]} - \bar{\rho}_{[b]}\big(\Delta v_{[b]} + 3\dot{\psi}\big) = 0 \,, \qquad \dot{v}_{[b]} + \mathcal{H}v_{[b]} - \phi = 0 \,, \tag{95a}$$

$$\delta\dot{\rho}_{[\gamma]} + 4\mathcal{H}\delta\rho_{[\gamma]} - \frac{4}{3}\bar{\rho}_{[\gamma]}\big(\Delta v_{[\gamma]} + 3\dot{\psi}\big) = 0 \,, \qquad \dot{v}_{[\gamma]} - \frac{\delta\rho_{[\gamma]}}{4\bar{\rho}_{[\gamma]}} - \phi = 0 \,. \tag{95b}$$

The equations presented above completely determine the evolution of the linearized cosmological perturbations. Their exact solution can be obtained only numerically. In the following section we find the approximate analytic form of the solution in various dynamical regimes. This will enable us to determine the qualitative influence of LV on the power spectra. The numerical analysis is postponed till Sec. 6.

5 Cosmological perturbations: qualitative analysis

Consider the mode with a given conformal wavenumber k. As usual, its evolution will be different depending on whether k is smaller or larger than the expansion rate $\mathcal{H}$. Coupling between DM and khronon gives rise to a second dynamical scale crucial for the mode evolution. Substituting Eq. (94) into Eq. (93a), we notice that the dynamics of the mode depends on the ratio between k and

$$k_Y \equiv \left(\frac{Y\bar{\rho}_{[dm]}a^2}{\alpha(1-Y)M_0^2}\right)^{1/2} \,. \tag{96}$$

This new scale is directly related to the density of DM and determines the critical wavenumber below which the effects of LV are screened (see discussion in Sec. 3). Factoring out the explicit time dependence we can write,

$$k_Y = \frac{k_{Y,0}}{\sqrt{a(\tau)}}\,, \qquad k_{Y,0} \equiv H_0 \left[\frac{3Y\Omega_{dm}}{\alpha(1-Y)}\left(1+\frac{\alpha\mathcal{B}}{2}\right)\right]^{1/2}\,, \tag{97}$$

where H_0, Ω_{dm} are the present-day Hubble constant and DM density fraction; the current value of the scale factor has been normalized to one, $a(\tau_0) = 1$. Note that under the assumption $\alpha \ll Y$ the present screening scale $k_{Y,0}$ is parametrically higher than the Hubble rate H_0. The hierarchy between k_Y and $\mathcal{H}$ persists during the whole matter dominated epoch and most of the radiation domination, see Fig. 1. Thus, the time evolution of a mode with

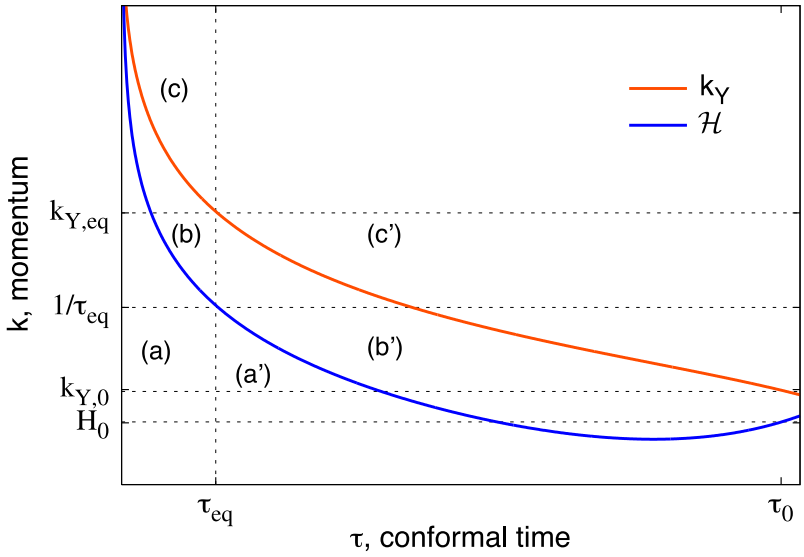

Figure 1: Time dependence of the dynamical scales determining the evolution of the cosmological perturbations. τ_{eq} is the time of radiation–matter equality and τ_0 — the present time. See the main text for other notations.

given k can be divided into the following regimes:

(a) superhorizon modes, $k < \mathcal{H}$, radiation dominated universe,

(a') superhorizon modes, $k < \mathcal{H}$, matter dominated universe,

(b) subhorizon modes with $\mathcal{H} < k < k_Y$, radiation dominated universe,

(b') subhorizon modes with $\mathcal{H} < k < k_Y$, matter dominated universe,

(c) subhorizon modes with $\mathcal{H} < k_Y < k$, radiation dominated universe,

(c') subhorizon modes with $\mathcal{H} < k_Y < k$, matter dominated universe.

To find the solution of the linear equations we use the following strategy. We first consider the formal limit $\alpha, \beta, \lambda \to 0$ suggested by the constraints on the khronon (aether) parameters listed in Sec. 2; at the same time we keep the parameter Y fixed. From (93a) one sees that in this limit the khronon is tightly coupled to the DM velocity, $\chi = v_{[dm]}$. Substituting this into the rest of equations we find that they take the standard GR form. Thus, to this approximation all perturbations, in particular the gravitational potentials ϕ and ψ, behave as in GR. At the next step we allow for finite α, β, λ (assuming all of them to be of the same order) and substitute the GR values for ϕ, ψ into Eqs. (93) to find the khronon and DM fluctuations. Finally, we find the corrections to ϕ, ψ by inserting χ, $v_{[dm]}$, $\delta\rho_{[dm]}$ into the Einstein's equations (91).

This logic has the caveat that in the limit $\alpha, \beta, \lambda \to 0$ the screening scale k_Y diverges. Thus, the above perturbative scheme is not applicable in cases *(c)* and *(c')* where the momentum k is parametrically large. Those cases will require a different approach.

5.1 Regime *(a)*: $k < \mathcal{H}$ during radiation domination

For the superhorizon modes, we can neglect all terms with spatial Laplacians and consider to leading order $\phi = \phi_\gamma = const$. At the radiation domination stage the scale factor depends linearly on the conformal time,

$$a(\tau) = A_\gamma \tau, \quad A_\gamma = \sqrt{\Omega_\gamma} H_0 \,, \tag{98}$$

where Ω_γ is the present fraction of the radiation density. Substituting this into Eqs. (93a), (94) and setting the constant of integration in (94) to zero, which amounts to the absence of initial velocities[21], we obtain,

$$\ddot{\chi} + \frac{2\dot{\chi}}{\tau} + \left[\frac{2\mathcal{B}}{\tau^2} + \frac{k_{Y,0}^2}{A_\gamma \tau}\right]\chi = \left[\frac{(1+\mathcal{B})}{\tau} + \frac{k_{Y,0}^2}{2A_\gamma}\right]\phi_\gamma \,. \tag{99}$$

This equation has a solution

$$\chi = \frac{\phi_\gamma}{2}\tau \,. \tag{100}$$

From (94) we find that it corresponds to

$$v_{[dm]} = \chi = \frac{\phi_\gamma}{2}\tau \,. \tag{101}$$

This is the standard expression for the perturbation of DM velocity in the adiabatic mode and we see that the khronon evolves coherently with the DM fluid. Note that this solution is completely insensitive to the parameter Y setting the strength of LV in DM. The corresponding DM density contrast in the adiabatic mode is [43] (see also Appendix A),

$$\delta_{[dm]} \equiv \frac{\delta\rho_{[dm]}}{\bar{\rho}_{[dm]}} = -\frac{3\phi_\gamma}{2} \,. \tag{102}$$

[21] Even if the initial velocities are present, their effect decays with time.

Inserting (101) into the Einstein's equations (91) one can find the corrections to the gravitational potentials induced by the khronon. Clearly, these corrections are suppressed by the parameters α, β, λ and we are not going to analyze them in detail. Let us just note that Eq. (91d) implies the appearance of a small anisotropic stress,

$$\frac{\phi - \psi}{\phi} = \frac{3\beta}{2} \,. \tag{103}$$

To determine whether the adiabatic mode (101) is an attractor, we search for the solution of the homogeneous equation, i.e. Eq. (99) with vanishing r.h.s. This can be found in terms of Bessel functions,

$$\chi^{(a)}_{hom}(\tau) = \frac{\chi^{(a)}_1}{\sqrt{\tau}} J_\nu\left(\frac{2k_{Y,0}}{\sqrt{A_\gamma}}\sqrt{\tau}\right) + \frac{\chi^{(a)}_2}{\sqrt{\tau}} Y_\nu\left(\frac{2k_{Y,0}}{\sqrt{A_\gamma}}\sqrt{\tau}\right) \,, \qquad \nu = \sqrt{1-8\mathcal{B}} \,, \tag{104}$$

where $\chi^{(a)}_{1,2}$ are arbitrary coefficients. Recall that we restrict to $0 \leq Y < 1$, in which case $k_{Y,0}$ is real and thus $\chi^{(a)}_{hom}$ oscillates and decays at late times as $\tau^{-3/4}$. In this case the adiabatic solution (100) is an attractor. For negative Y, $k_{Y,0}$ is imaginary and the solution (104) contains an exponentially growing part signaling the instability of the system. We have already encountered this instability when we studied the Newtonian limit in Sec. 3. For the rest of the paper, we will only consider positive values of Y.

At early times, $\tau \ll A_\gamma/k^2_{Y,0}$, the first term in (104) evolves as τ^q with

$$q = \frac{-1+\sqrt{1-8\mathcal{B}}}{2} \,. \tag{105}$$

For $\mathcal{B} < -1$ it grows faster than the adiabatic mode (100) and, depending on the initial conditions, may dominate over it. This corresponds to an intrinsic instability of the khronon (not to confuse with the instability discussed in the previous paragraph) [42, 22]. It is curious that the coupling to DM cuts off this instability at $\tau \sim A_\gamma/k^2_{Y,0}$, and makes the apparently growing mode decay. In this paper we will assume that the initial conditions for the cosmological perturbations are sufficiently close to adiabatic, so that this mode never becomes dominant.

5.2 Regime *(a')*: $k < \mathcal{H}$ during matter domination

During matter domination the scale factor grows as

$$a(\tau) = A_m \tau^2 \,, \qquad A_m = (\Omega_{dm} + \Omega_b) H_0^2/4 \,, \tag{106}$$

where Ω_b is the baryon density fraction today. At zeroth order, the superhorizon amplitude of the gravitational potential is now $\phi_m = \frac{9}{10}\phi_\gamma$. After substituting this into Eqs. (93a), (94) and neglecting the terms with spatial Laplacians one obtains the following equation:

$$\ddot{\chi} + \frac{4\dot{\chi}}{\tau} + \left[2(1+3\mathcal{B}) + \frac{k^2_{Y,0}}{A_m}\right]\frac{\chi}{\tau^2} = \left[2(1+\mathcal{B}) + \frac{k^2_{Y,0}}{3A_m}\right]\frac{\phi_m}{\tau} \,. \tag{107}$$

Here we have neglected the integration constant in (94) which corresponds to a decaying contribution. The adiabatic mode

$$v_{[dm]} = \chi = \frac{\phi_m}{3}\tau \tag{108}$$

is a solution. To check its stability consider the solution of the homogeneous equation,

$$\chi^{(a')}_{hom}(\tau) = \chi^{(a')}_1 \tau^{r_+} + \chi^{(a')}_2 \tau^{r_-} \ , \qquad r_\pm = \frac{1}{2}\Big[-3 \pm \sqrt{1 - 24\mathcal{B} - \frac{4k^2_{Y,0}}{A_m}}\Big] \ . \tag{109}$$

For all parameters of interest the expression under the square root is negative and $\chi^{(a')}_{hom}$ describes decaying oscillations. The adiabatic mode (108) gives rise to the anisotropic stress

$$\frac{\phi - \psi}{\phi} = \frac{5\beta}{3} \ . \tag{110}$$

Comparing to (103) and taking into account the ratio between ϕ_m and ϕ_γ we see that the absolute difference $(\phi - \psi)$ actually stays constant at the transition from radiation to matter domination.

5.3 Regimes *(b)*, *(c)*: $k > \mathcal{H}$ during radiation domination

The gravitational potentials decay rapidly inside the horizon during the radiation domination, so we can neglect them in Eqs. (93a), (94). The latter then takes the form,

$$v_{[dm]} = -\frac{Y}{1-Y}\,\chi + \frac{v^{(0)}}{\tau(1-Y)} \ , \tag{111}$$

where $v^{(0)}$ is a constant. By matching (111) approximately to (101) at horizon crossing $k\tau \sim 1$ we find $v^{(0)} \approx \phi_\gamma / 2k^2$. Substitution into (93a) gives

$$\ddot{\chi} + \frac{2\dot{\chi}}{\tau} + \left[\mathcal{C}^2 k^2 + \frac{k^2_{Y,0}}{A_\gamma \tau}\right]\chi = \frac{k^2_{Y,0}\phi_\gamma}{2A_\gamma k^2 \tau^2} \ , \tag{112}$$

where we have neglected the terms related to the Hubble parameter $\mathcal{H}$ in the square bracket.

For $k \ll k_{Y,0}/\sqrt{A_\gamma \tau}$ (regime *(b)*) the solution reads,

$$\chi(\tau) = \frac{\phi_\gamma}{2k^2\tau} + \frac{\chi^{(b)}_1}{\sqrt{\tau}} J_1\left(\frac{2k_{Y,0}}{\sqrt{A_\gamma}}\sqrt{\tau}\right) + \frac{\chi^{(b)}_2}{\sqrt{\tau}} Y_1\left(\frac{2k_{Y,0}}{\sqrt{A_\gamma}}\sqrt{\tau}\right) \ . \tag{113}$$

This is a sum of a monotonically decreasing mode and damped oscillations. The same structure is inherited by $v_{[dm]}$ through Eq. (111) and eventually, due to Eq. (93b), leads to

the standard logarithmic growth of the DM density contrast (the LV effects are screened), accompanied by damped oscillations,

$$\delta_{[dm]} \approx -\frac{3\phi_\gamma}{2} - \frac{\phi_\gamma}{2}\log(k\tau) + (\text{damped oscillations})\,. \tag{114}$$

For $k \gg k_{Y,0}/\sqrt{A_\gamma \tau}$ (regime *(c)*) the formal perturbative expansion in α, β, λ breaks down, as the corrections proportional to αk^2 in the Einstein's equations (91) may become large in this regime (recall that $k_{Y,0}$ is inversely proportional to $\sqrt{\alpha}$). Nevertheless, we can rely on the fact that during the radiation domination the DM perturbations are subdominant. It is reasonable to assume that this is also true for the khronon fluctuations which are coupled to DM. Then the dynamics are still dominated by the sound waves in the hot plasma that wash out the gravitational potentials. Therefore, Eq. (111) for the velocity of DM and Eq. (112) for the khronon still hold. Moreover, in the latter equation one can neglect the second term in the square brackets and the r.h.s. and obtain,

$$\chi(\tau) = \chi_1^{(c)}\frac{\sin(\mathcal{C}k\tau)}{\tau} + \chi_2^{(c)}\frac{\cos(\mathcal{C}k\tau)}{\tau}\,. \tag{115}$$

Using (111), (93b) we obtain for the density contrast,

$$\delta_{[dm]} = \text{const} - \frac{\phi_\gamma}{2(1-Y)}\log\tau + \frac{k^2 Y\chi_1^{(c)}}{1-Y}\mathbf{Si}(\mathcal{C}k\tau) + \frac{k^2 Y\chi_2^{(c)}}{1-Y}\mathbf{Ci}(\mathcal{C}k\tau) \tag{116}$$

where $\mathbf{Si}(x)$ and $\mathbf{Ci}(x)$ are the integral sine and cosine,

$$\mathbf{Si}(x) = \int_0^x d\xi\,\frac{\sin\xi}{\xi}, \quad \mathbf{Ci}(x) = \gamma + \ln(x) + \int_0^x d\xi\,\frac{\cos\xi - 1}{\xi}\,.$$

Notice that the coefficient in front of the logarithmic term has been renormalized by the LV effects. The last two terms again describe damped oscillations.

The oscillations in the DM density and velocity field found above could potentially provide an interesting signature of the model. Unfortunately, the numerical solution in Sec. 6 shows that they are rather weak and can leave a noticeable imprint only at very short wavelengths that are presently in the non-linear regime. It is unclear whether such effects can be observed.

5.4 Regimes *(b')*, *(c')*: $k > \mathcal{H}$ during matter domination

We finally consider the evolution of subhorizon modes at the matter dominated epoch. If one neglects the effects of LV, the Newtonian potential stays constant, $\phi = \phi_{m,k}$, where the subscript k indicates the dependence on the wavenumber. Neglecting in (94) the integration constant that gives a rapidly decaying contribution and substituting the resulting expression for the velocity into (93a) we obtain

$$\ddot{\chi} + \frac{4\dot{\chi}}{\tau} + \left[\mathcal{C}^2k^2 + \frac{k_{Y,0}^2}{A_m\tau^2}\right]\chi = \left[2(1+\mathcal{B}) + \frac{k_{Y,0}^2}{3A_m}\right]\frac{\phi_{m,k}}{\tau}\,. \tag{117}$$

For $k \ll k_{Y,0}/\sqrt{A_m}\,\tau$ (regime *(b')*) the solution is

$$\chi = \left[\frac{6A_m(1+\mathcal{B})+k_{Y,0}^2}{12A_m+3k_{Y,0}^2}\right]\phi_{m,k}\,\tau + \chi_1^{(b')}\tau^{p_+} + \chi_2^{(b')}\tau^{p_-}\ , \qquad p_\pm = -\frac{3}{2} \pm \sqrt{\frac{9}{4}-\frac{k_{Y,0}^2}{A_m}}\ . \tag{118}$$

The definitions of $k_{Y,0}$, A_m in (97), (106) imply that $k_{Y,0}^2/A_m \sim Y/\alpha$ is parametrically large. Thus the last two terms in the above solution describe quickly decaying oscillations and one is left with the attractor behavior (cf. (108)),

$$v_{[dm]} \approx \chi \approx \frac{\phi_{m,k}}{3}\tau\ . \tag{119}$$

The velocity perturbation has exactly the same form as in GR, so we again conclude that in this regime the LV effects are essentially screened. The corresponding density contrast is found from (93b) and exhibits the standard quadratic growth in time,

$$\delta_{[dm]} \approx -\frac{(k\tau)^2}{6}\phi_{m,k}\ . \tag{120}$$

It is instructive to go one step further and consider the corrections to the gravitational potentials induced by the khronon[22]. From Eqs. (91c), (91d) we find

$$\phi = \phi_{m,k}\left(1+\frac{5}{84}(\beta+\lambda)(k\tau)^2\right)\ , \qquad \psi = \phi_{m,k}\left(1-\frac{5\beta}{3}+\frac{5}{84}(\beta+\lambda)(k\tau)^2\right)\ . \tag{121}$$

These expressions are valid up to linear order in α, β, λ. We observe that the corrections, though small, grow with time. Eventually, when k_Y red-shifts down to k, they become of order Y: this follows from the estimate $(k_Y\tau)^2 \sim Y/\alpha$. The suppression of the corrections by the small parameters α, β, λ disappears, which suggests the break down of our perturbative scheme by the end of the regime *(b')*. Note however, that the anisotropic stress remains constant and given by Eq. (110) during this stage.

For $k \gg k_{Y,0}/\sqrt{A_m}\,\tau$ (regime *(c')*) one can show that the corrections to the gravitational potentials are not proportional to the expansion parameters α, β, λ, so the perturbative calculation fails. Thus we have to solve the coupled Einstein–khronon–DM equations self-consistently. One notices that (91c), (91d), (93a), (93c) form a closed system of equations for ϕ, ψ, χ, $v_{[dm]}$. The educated guess of a power-law behavior yields the growing mode,

$$\psi = \phi = \tilde{\phi}_{m,k}\,\tau^{\varkappa}\ , \tag{122a}$$

$$\chi = \frac{k_{Y,0}^2\tilde{\phi}_{m,k}}{\mathcal{C}^2k^2A_m(\varkappa+3)}\,\tau^{\varkappa-1}\ , \tag{122b}$$

$$v_{[dm]} = \frac{\tilde{\phi}_{m,k}}{(1-Y)(\varkappa+3)}\,\tau^{\varkappa+1}\ , \tag{122c}$$

[22]There are also corrections to $\delta_{[dm]}$, $v_{[dm]}$ at the same order which we do not consider here.

where

$$\varkappa = -\frac{5}{2} + \sqrt{\frac{25}{4} + \frac{6Y}{1-Y}\frac{\Omega_{dm}}{\Omega_{dm}+\Omega_b}}\,, \tag{123}$$

and we have neglected the corrections of order α, β, λ. The mode normalization $\tilde{\phi}_{m,k}$ can be determined by matching (122) to the solution before crossing the screening horizon $k = k_Y$.

Substituting (122c) into (93b) we find the behavior of the DM density contrast,

$$\delta_{[dm]} = -\frac{k^2\tilde{\phi}_{m,k}}{(1-Y)(\varkappa+3)(\varkappa+2)}\,\tau^{\varkappa+2}\,. \tag{124}$$

One observes that $\delta_{[dm]}$ grows faster than in GR, implying the accelerated growth of structure. The power-law (124) coincides with the results in Sec. 3.2 (see Eq. (54)) if we neglect the baryon contribution, i.e. set $\Omega_b = 0$, and take into account the relation between the conformal and physical time, $\tau^3 \propto t$.

It is interesting to study the perturbations of the baryonic component. From (95a) we find,

$$\delta_{[b]} \equiv \frac{\delta\rho_{[b]}}{\bar{\rho}_{[b]}} = -\frac{k^2\tilde{\phi}_{m,k}}{(\varkappa+3)(\varkappa+2)}\,\tau^{\varkappa+2}\,. \tag{125}$$

Thus the baryon density contrast grows at the same rate as that of DM, but with an overall amplitude suppressed by a Y-dependent factor,

$$\frac{\delta_{[b]}}{\delta_{[dm]}} = 1 - Y\,. \tag{126}$$

This behavior has a simple physical explanation: baryons do not feel the enhanced gravitational acceleration experienced by DM. Therefore it takes them longer to react to the inhomogeneities of the gravitational potential and their density perturbations stay behind those of DM.

The anisotropic stress is found from (91d) and reads,

$$\frac{\phi-\psi}{\phi} = \beta\cdot\frac{k_{Y,0}^2}{\mathcal{C}^2 A_m k^2\tau^2}\,. \tag{127}$$

Notice that the second factor on the r.h.s. is always smaller than 1 in the considered regime, so that the anisotropic stress is still suppressed by β. Moreover, it decays with time as τ^{-2}.

Finally, it is straightforward to check that the solution (122), (124), (125) satisfies the remaining Einstein's equations (91a), (91b).

5.5 Qualitative analysis of the power spectra

The previous analysis allows us to sketch the qualitative picture of the effects due to LV in DM in the observed power spectra of DM and baryon density perturbations. From Fig. 1 we see that the modes with different k go through a different sequence of the dynamical regimes described before.

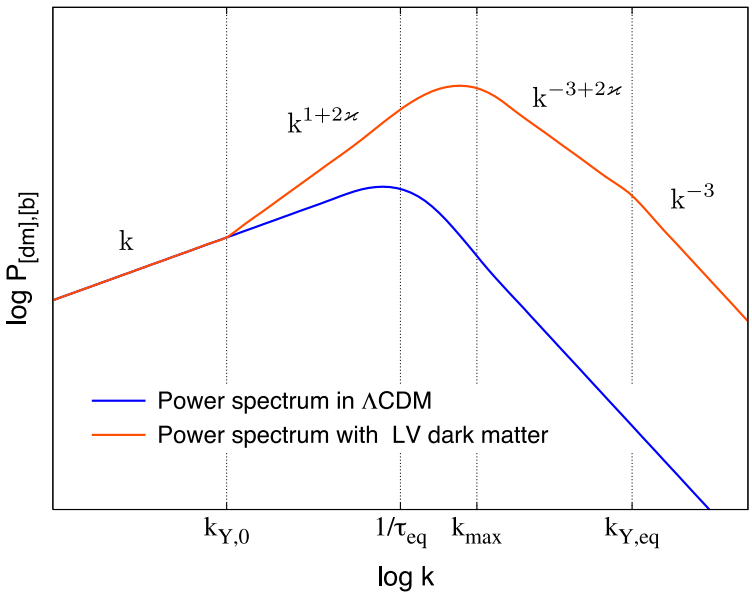

Figure 2: Schematic representation of the matter power spectrum in the LV dark matter model (upper curve) compared to the power spectrum in ΛCDM (lower curve). The same qualitative behavior is common to the dark matter and baryons. The quantities $k_{Y,0}$, $k_{Y,eq}$, $\varkappa$ are defined in (97), (128), (123). The figure corresponds to the case $k_{Y,0} < 1/\tau_{eq}$.

- The modes with $k < k_{Y,0}$ always stay in the regime where the LV effects are essentially screened. In this range the power spectrum has the same dependence on k as in ΛCDM.

- The modes with $k_{Y,0} < k < k_{Y,eq}$, where

$$k_{Y,eq} \equiv \frac{k_{Y,0}}{\sqrt{a(\tau_{eq})}} = k_{Y,0}\sqrt{\frac{\Omega_{dm}+\Omega_b}{\Omega_\gamma}}, \tag{128}$$

  is the screening scale at the radiation–matter equality, enter into the regime of unscreened LV at the matter dominated stage. Let us denote the moment of the "screening horizon" crossing by $\tau_Y(k)$,

$$\tau_Y(k) \equiv \frac{k_{Y,0}}{\sqrt{A_m}k} \ .$$

  Between τ_Y and τ_0 the density contrasts exhibit the anomalous growth (124), (125). Thus they are enhanced by a factor $(\tau_0/\tau_Y)^\varkappa$ leading to the increase of the power spectra by a factor $\propto k^{2\varkappa}$ in this range of momenta.

- Finally, the modes with $k > k_{Y,eq}$ enter in the unscreened regime already during radiation domination. Modulo the small damped oscillations mentioned in Sec. 5.3, the net

effect of LV on these modes is the overall enhancement by the factor $(\tau_0/\tau_{eq})^{\varkappa}$. This factor does not depend on the mode momentum, so the slope of the spectrum remains as in ΛCDM.

This picture is summarized in Fig. 2. For the sake of the schematic representation we have assumed a flat spectrum for the initial perturbations, neglected the logarithmic growth of the perturbations during the radiation domination together with the effects of the cosmological constant. Note that the change in the slope of the power spectrum depends only on the parameter Y describing LV in DM, while the range of scales where this change occurs is determined both by Y and the khronon parameters α, β, λ.

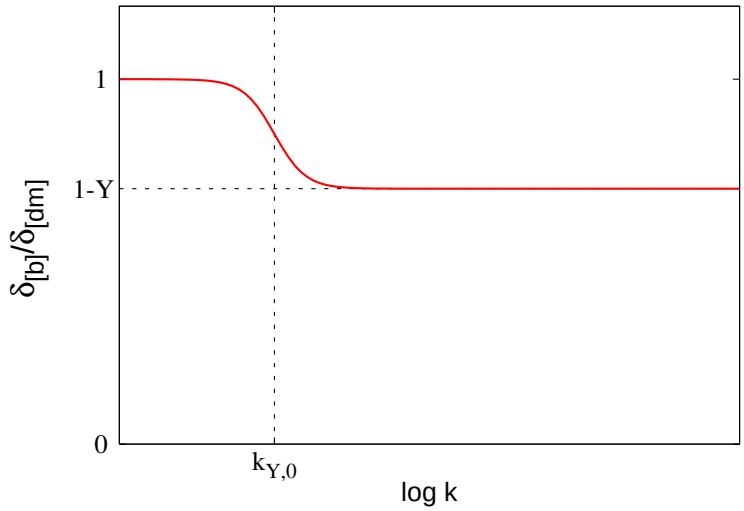

Figure 3: Ratio between the density contrasts of baryons and dark matter (qualitative plot).

Figure 2 corresponds to the situation when the ratio Y/α is moderately large, so that $k_{Y,0}$ is smaller than $1/\tau_{eq}$, the Hubble rate at the radiation–matter equality that sets the position of the maximum of the power spectrum in ΛCDM. In this case the change in the slope of the power spectrum leads also to the shift of its maximum. Indeed, in the log-log scale the standard ΛCDM power spectrum in the vicinity of the maximum can be written as

$$\log P^{\Lambda CDM} = A_1 - A_2(\log k\tau_{eq})^2 \ ,$$

where $A_{1,2}$ are some constants. The additional enhancement due to LV adds a linear contribution on top of it,

$$\log P = \log P^{\Lambda CDM} + 2\varkappa \log k \ .$$

Differentiating this expression with respect to k we obtain the new position of the maximum,

$$\log k_{max} = \log 1/\tau_{eq} + \varkappa/A_2 \ . \qquad (129)$$

We conclude that the shift is linearly proportional to $\varkappa$.

If $k_{Y,0} > 1/\tau_{eq}$, which happens for an extreme hierarchy between Y and α, the position of the maximum of the power spectrum is not modified. However, the change in the slope is still present providing the signature of LV.

The second qualitative effect of LV in DM is the appearance of the baryon — DM bias (126) for the modes undergoing the anomalous growth, i.e. all modes with wavenumbers larger than $k_{Y,0}$. For smaller k the density contrasts of the baryons and DM are equal. This results in the scale dependence of the bias shown in Fig. 3. It would be interesting to understand how this effect could be constrained by observations.

Finally, at non-zero value of the parameter β the model is also characterized by the anisotropic stress. Its present-day value is independent of k for $k < k_{Y,0}$ where it is given by Eq. (110). At larger wavenumbers it falls off as k^{-2} according to Eq. (127).

The qualitative analysis of this section is confirmed by the numerical calculations, to which we proceed now.

6 Cosmological perturbations: numerics

The study of the effects of LV in the DM sector yielded the modified linearized equations for cosmological perturbations (91), (93), (95). In this section we will solve these equations numerically for different sets of LV parameters and confirm the modifications in the growth of perturbations uncovered in Sec. 5. The density fractions of the cosmological constant, DM, baryons and radiation are taken to be

$$\Omega_\Lambda = 0.75, \quad \Omega_{dm} = 0.2, \quad \Omega_b = 0.05, \quad \Omega_\gamma = 5 \cdot 10^{-5}.$$

We neglect the interaction between baryons and radiation as well as the effects of neutrinos. As our goal is to compare the evolution of perturbations in models of LV DM with ΛCDM, we also find the evolution of perturbations in ΛCDM within the same approximations[23]. The details of the numerical procedure are presented in Appendix A.

The first set of parameters we consider is

$$\alpha = 0.02\ , \quad \beta = 0.01\ , \quad \lambda = 0.01\ , \quad Y = 0.2\ . \tag{130}$$

This choice satisfies the PPN[24], BBN and gravitational radiation constraints [14, 18]. The initial conditions correspond to the adiabatic mode, and for illustration purposes the initial value of ϕ is normalized to 1 for all modes. Figure 4 shows the dependence of the Newton potential on conformal time for the choice (130) and for ΛCDM for several modes with different values of momentum. The difference $(\phi - \psi)$ is also shown. We see that perturbations of the gravitational potential are enhanced at late times as compared to ΛCDM. The enhancement is stronger for shorter modes that enter earlier into the regime where the LV effects are not screened. Note that the present-day screening scale corresponding to the choice (130) is

[23]The corresponding equations follow from (91), (93b), (93c) by setting $Y = \alpha = \beta = \lambda = 0$, $\chi = v_{[dm]}$.

[24]Recall that $\alpha = 2\beta$ case avoids the PPN bounds.

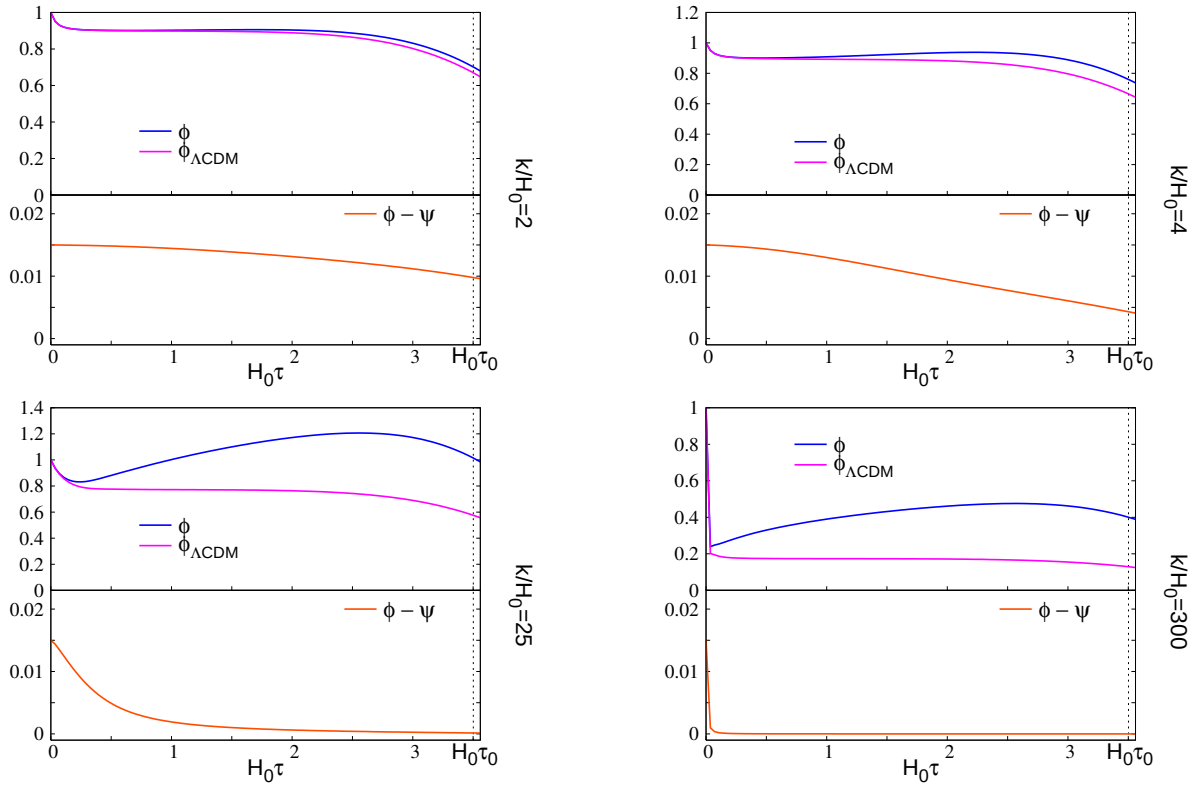

Figure 4: Dependence of the gravitational potentials on conformal time for modes with momenta $k/H_0 = 2,\ 4,\ 25,\ 300$. The LV parameters of the model are $\alpha = 0.02$, $\beta = 0.01$, $\lambda = 0.01$, $Y = 0.2$. The standard ΛCDM result is shown for comparison. Dashed vertical lines mark the present conformal time $\tau_0 = 3.5 H_0^{-1}$.

$k_{Y,0} = 2.77\, H_0$. On the other hand, the difference between the two gravitational potentials $(\phi - \psi)$ which is initially of order 10^{-2} decreases once the mode enters inside the screening horizon. Note that the overall amplitude 10^{-2} for long wavelength modes agrees with the estimate $(\phi - \psi)/\phi \sim \beta$ obtained in the previous section.

In Fig. 5 we plot the total (DM plus baryons) density contrast in the present model divided by its value in ΛCDM. As expected from the analysis of Sec. 5 (or simply from the enhancement of the gravitational perturbations), the growth of structures increases at recent times in a wide range of momenta. The relative effect is stronger for shorter modes and can be large for our choice of parameters.

In Sec. 5.3 we found that the subhorizon DM perturbations exhibit damped oscillations during the radiation-dominated epoch. To study this effect we plot in Fig. 6 the early-time behavior of the longitudinal component of the DM velocity (see Eq. (90) for the definition) and the DM density contrast; the latter is normalized to the density contrast in ΛCDM. One observes that the oscillations are rather weak in the velocity and are almost completely

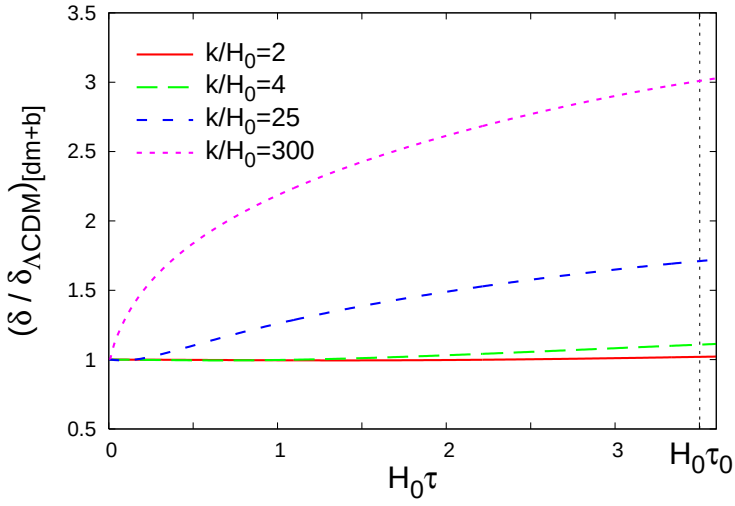

Figure 5: Ratio of total density contrasts between the model with LV DM and ΛCDM versus time for several values of the mode momentum k. The parameters are the same as for Fig. 4. τ_0 is the present conformal time.

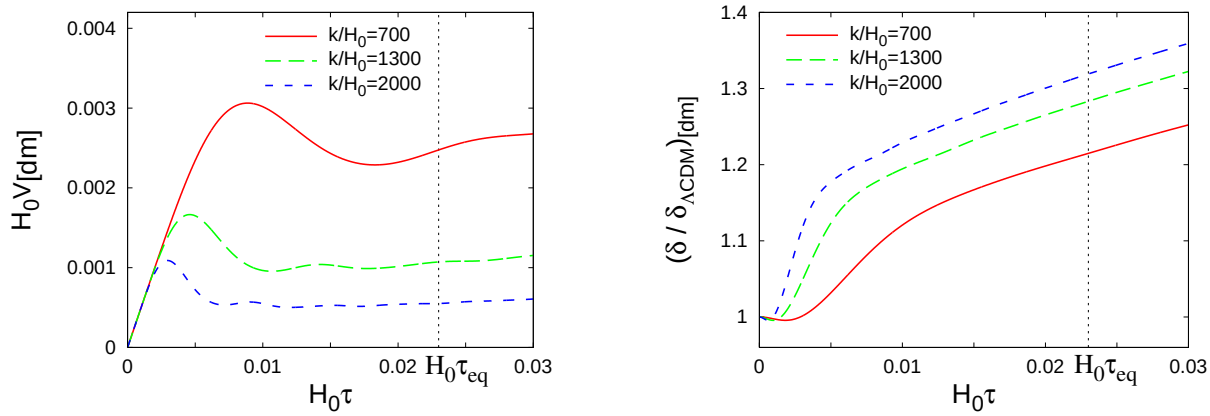

Figure 6: Time-dependence of the longitudinal component of the DM velocity (left panel) and the DM density contrast (right panel) for several subhorizon modes at the radiation-dominated epoch. The dashed vertical line marks the time of radiation – matter equality, $\tau_{eq} \approx 0.023 H_0^{-1}$. The parameters of the model are the same as for Fig. 4.

washed out in the density contrast. Besides, for the velocity they are perceptible only in very short modes that have by now entered into the non-linear regime. Thus it is unclear whether the oscillations can have an impact on any observable.

We now consider the effects of different sets of parameters on the spectra of perturbations

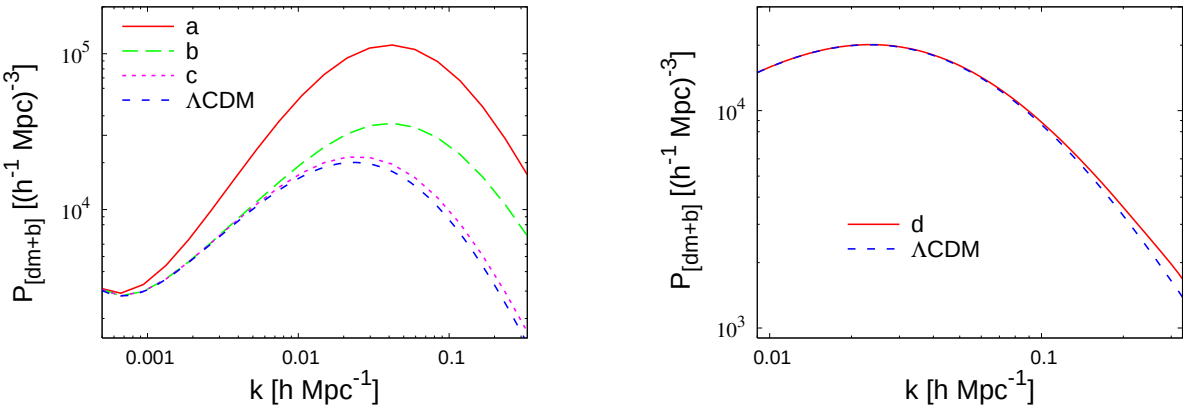

Figure 7: Matter power spectrum for several values of the parameters listed in Table 1. The case of ΛCDM is shown for comparison.

at the present moment of time. The different choices are listed in Table 1 together with the corresponding values of the screening scales $k_{Y,0}$ and $k_{Y,eq}$ (see Eqs. (97), (128) for definitions). All parameter choices are consistent with the gravitational tests described in Sec. 2. The initial spectrum is taken to be flat with the same normalization in all cases.

	α	β	λ	Y	$k_{Y,0}$ (h Mpc^{-1})	$k_{Y,eq}$ (h Mpc^{-1})
a	$2 \cdot 10^{-2}$	10^{-2}	10^{-2}	0.2	$9.2 \cdot 10^{-4}$	$6.5 \cdot 10^{-2}$
b	$2 \cdot 10^{-4}$	10^{-4}	10^{-4}	0.2	$9.1 \cdot 10^{-3}$	0.65
c	$2 \cdot 10^{-4}$	10^{-4}	10^{-4}	0.02	$2.6 \cdot 10^{-3}$	0.18
d	10^{-7}	0	10^{-7}	0.2	0.41	29

Table 1: The values of the parameters used in numerical simulations.

The comparison between the matter power spectrum in the LV models and in ΛCDM is shown in Fig. 7. The left panel shows the cases when the present screening momentum $k_{Y,0}$ is lower than k_{max} — the position of the power spectrum maximum. We clearly see the change in the slope of the spectrum in the interval $k_{Y,0} < k < k_{Y,eq}$ accompanied by the shift of the position of the maximum. The effect is significant for values of the parameter Y as low as a few per cent, which suggests that these values can be tested observationally. The right panel shows the situation when $k_{Y,0}$ is larger than k_{max}, corresponding to very small values of the khronon parameters α, β, λ and relatively strong LV in DM, see Table 1. The position of the maximum does not move in this case but the change in the slope is still visible.

Figure 8 shows the ratio between the amplitudes of perturbations in the baryonic and DM components. As expected from the analytic considerations of Sec. 5, this ratio drops from 1 at $k < k_{Y,0}$ to $(1 - Y)$ at larger momenta implying a scale dependent bias between baryons and DM.

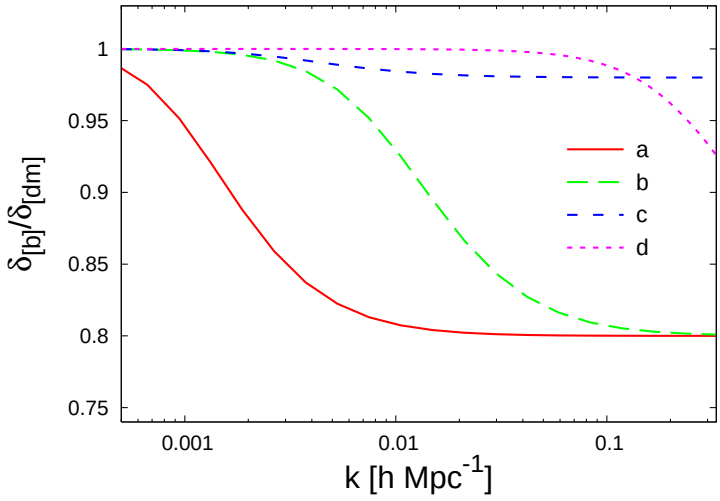

Figure 8: Ratio between the amplitudes of perturbations in the baryonic and dark matter components. The curves correspond to the parameters listed in Table 1.

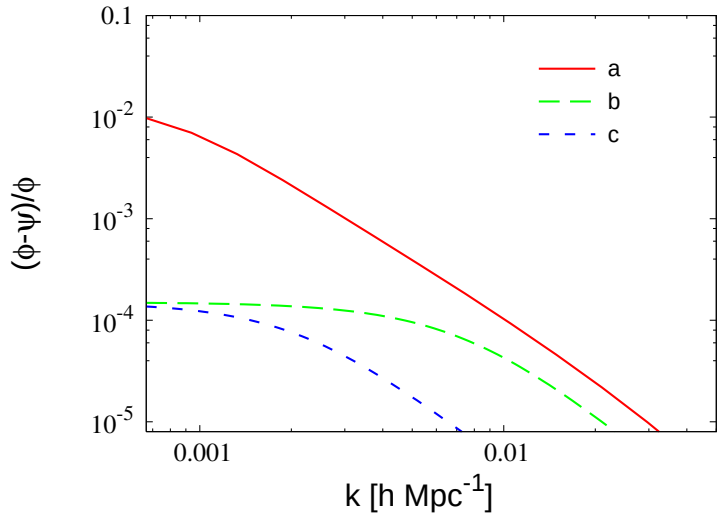

Figure 9: Relative difference between the two scalar gravitational potentials for several choices of parameters listed in Table 1.

Finally, Fig. 9 presents the k-dependence of the "relative anisotropic stress" — the difference between the two gravitational potentials ϕ and ψ in the conformal Newton gauge, normalized to ϕ. We observe that at small momenta it has a plateau with the magnitude set by the parameter β. The plateau extends up to $k \approx k_{Y,0}$, beyond which the anisotropic stress drops as the approximate power–law k^{-2}. All this is in agreement with the analytic

estimates of Sec. 5. Note that the persistence of the anisotropic stress up to relatively large momentum, $k_{Y,0} \gg H_0$, is a peculiar signature of the present model that contrasts with the more common situation where the anisotropic stress quickly decays for subhorizon modes. Besides, the anisotropic stress is present at early times even for adiabatic initial conditions. This distinguishes the present model from Lorentz-invariant models of modified gravity, such as $f(R)$ [44] or DGP [45] theories, where the anisotropic stress is generated only at a recent epoch [46].

7 Summary and discussion

In this paper we have studied the possibility to test the Lorentz invariance of dark matter (DM) with cosmological observations. Our description is based on the Einstein-aether/ khronometric model, which provides an effective description of Lorentz invariance violation (LV) in gravitational relativistic theories. In those models, LV is encoded in a new field (aether) whose expectation value determines a local preferred frame. We considered DM as described by a pressureless fluid, and generalized its dynamics to include the LV effects. Those effects amount to different couplings between DM and the aether field. For cosmological perturbations in the linear regime all the LV effects in the DM sector can be summarized in a single parameter Y. This constant is to be added to the parameters of the aether sector (see Eqs. (2), (3) and (8)), which are constrained by local tests of gravity. We considered the Newtonian limit of the model and demonstrated that LV implies modification of the inertial mass for small DM halos thus leading to the violation of the equivalence principle. For large halos this effect is screened by a variant of the chameleon mechanism. Additionally, we pointed out the presence of a velocity-dependent interaction; however, its role in the evolution of the Universe at large scales is negligible.

The homogeneous expansion history of the Universe for LV DM was found to be exactly the same as in ΛCDM. However, the evolution of linear cosmological perturbations presents three major effects permitting us to distinguish between the two scenarios. The first effect is the accelerated growth of inhomogeneities for the modes affected by the violation of the equivalence principle. These are the modes that are short enough so that the chameleon mechanism does not switch on. This effect eventually leads to the increase in the slope of the matter power spectrum with respect to ΛCDM in a range of momenta. The enhancement depends only on the parameter Y, whereas the range of momenta is determined also by the aether parameters (cf. Fig. 7). The second effect is the appearance of a new bias between the fluctuations of dark and ordinary baryonic matter. Importantly, the bias exhibits scale-dependence already at the linear level (cf. Fig. 8). Finally, the model predicts non-zero anisotropic stress resulting in the difference between the perturbations of the two gravitational potentials in the conformal Newton gauge. While this effect is present already in the pure Einstein-aether/khronometric theory, the novel feature introduced by the aether – DM coupling is the persistence of the anisotropic stress with time in a wide range of momenta. As a consequence, its present-day power spectrum extends to wavelengths quite inside the current horizon (cf. Fig. 9).

A qualitative comparison between the predictions of the model and those of ΛCDM suggests that the existing data (including local tests of gravity) have the potential to constrain deviations from Lorentz invariance in DM at the level of a few per cent or even better, $Y \lesssim 0.01$. This limit depends on the parameters of the aether sector and may be stronger or weaker for certain regions in the parameter space. Detailed numerical simulations are required to set the precise bounds. This work is currently in progress.

It is worth comparing the signatures we found with the predictions of Lorentz invariant models where DM has unusual properties. A large class of models discussed in the literature [24, 25, 47, 48, 49, 50, 51] includes one or several light scalar fields mediating long-range interactions between DM particles, referred to as fifth-forces. Depending on the model, the range of the fifth-force may or may not depend on the DM density. The additional interaction implies violation of the equivalence principle in the DM sector, similarly to our model. As a consequence, models with a fifth-force can also exhibit an accelerated growth of matter perturbations, as well as scale-dependent bias between DM and baryons. However, the resulting shape of the power spectrum in these models is in general different from the one found in this paper. The main reason is the different time dependence of the screening scale for the fifth-force. For example, in the simplest case of a scalar with fixed mass μ the screening momentum — the analog of our $k_Y(\tau)$ — is set by $\mu\, a(\tau)$ and thus *grows* with time. This means that for a given mode the fifth-force is important at early times and becomes screened later. On the contrary, in our case $k_Y(\tau)$ *decreases* as $a(\tau)^{-1/2}$ and the modes enter into the regime of non-standard evolution at late epochs. This leads to quite different shapes of the transfer function and power spectrum in the two cases, compare Fig. 2 with Fig. 4 of [25].

One can envisage more complicated fifth-force models where the squared mass of the scalar field is proportional to the DM density. The screening scale in such a model will behave exactly as $k_Y(\tau)$ mimicking the effect of LV on the power spectrum. In this case one can try to distinguish between the two models by examining the relation between the anomalous growth index of perturbations and the bias factor. In the LV case this relation is set by Eqs. (123), (126), while in the fifth-force theories the formulas are more complicated, cf. Eqs. (3.11), (3.12) of [25]. The origin of this discrepancy lies in the different dynamics of the models. As discussed in Sec. 3, the violation of equivalence principle in our case is mainly due to the change in the *inertial* mass of the DM particles (Eq. (30a)), while their *gravitational* mass remains the same (Eq. (30c)). The gravitational potential produced by DM is just the usual one. Combined with the contribution of baryons it adds up to the total potential that appears as the same forcing term in the hydrodynamical equations both for baryons and DM (Eq. (30a) and the equivalent with $Y = 0$ for baryons). In other words, the bias between DM and baryons in the case of LV comes from the change of the inertial mass of DM. On the other hand, the standard fifth-force appears as an extra forcing term for the DM sector, without a modification of the inertial mass of DM. Thus the hydrodynamic equations for baryons and DM have different forcing terms with a complicated relation between them.

Another feature of our model that distinguishes it from other fifth-force theories is the presence of the anisotropic stress both at early and late times. However, this effect is rather

small and may be outside the reach of observations (cf. Fig. 9).

There are several interesting questions to explore in the physics of LV DM. For large scale structure, it would be interesting to go beyond linear theory and understand how LV affects the cosmological dynamics of DM at the non-linear level. This would allow us to extend our results to scales shorter than 100 Mpc, where new data can be used to constrain the model. For this, one can resort to analytic methods in the lines of [52, 53, 54, 55] or, alternatively, use N-body simulations. Another open direction is related to the finding [56] that the violation of equivalence principle by DM has pronounced effects on the tidal disruption of satellite galaxies. It seems promising to look for similar signatures at the level of galaxies and galaxy clusters in the model considered in this paper. One expects to encounter a rather rich dynamics, given that the model contains velocity-dependent interactions and automatically incorporates a chameleon mechanism that screens the deviations from the standard physics for large mass concentrations. This kind of study may lead to interesting bounds on the model, complementary to those discussed in the present work.

Acknowledgments We are grateful to Cedric Deffayet, Sergei Demidov, Sergey Dubovsky, Dmitry Gorbunov, Eugene Lim, Alexander Panin, Valery Rubakov, Roman Scoccimarro, Igor Tkachev, Alexey Toporensky, Shinji Tsujikawa and Andrea Wulzer for useful discussions. D.B. thanks CCPP of NYU for hospitality at the earlier stages of this work. M.I. and S.S. are grateful to the Institute of Theoretical Physics of EPFL for hospitality during the completion of this paper. This work was supported in part by the Swiss National Science Foundation, grant IZKOZ2 138892/1 of the International Short Visits Program (D.B.), the Grants of the President of Russian Federation NS-5590.2012.2 and MK-3344.2011.2 (M.I. and S.S.), the RFBR grants 11-02-92108 (S.S.), 11-02-01528 (S.S.), 12-02-01203 (S.S.) and by the Dynasty Foundation (M.I. and S.S.).

A Numerical procedure

The complete system of equations for the evolution of the cosmological perturbations in the model consists of Einstein's equations (91), equations for the khronon and DM (93) and the hydrodynamical equations for the ordinary matter (95). Not all of these equations are independent. For the numerical procedure we choose two Einstein's equations (91c), (91d). To these we add Eqs. (93a), (93c) for the evolution of the khronon and DM velocity. To close the system we have to evaluate the pressure term in (91c). Only the radiation component contributes into it. The two first-order equations (95b) governing its evolution can be reduced to one of second order,

$$\ddot{\delta}_{[\gamma]} - \frac{\Delta\delta_{[\gamma]}}{3} - \frac{4\Delta\phi}{3} - 4\ddot{\psi} = 0 \,,$$

where we have introduced the density contrast,

$$\delta_{[\gamma]} \equiv \frac{\delta\rho_{[\gamma]}}{\bar{\rho}_{[\gamma]}} \,.$$

Performing the Fourier decomposition, normalizing the present scale factor to one, $a(\tau_0) = 1$, and choosing the units such that the present Hubble parameter is equal to one, $H_0 = 1$, we obtain the final system of ordinary differential equations to be solved numerically:

$$\ddot{\psi} + \mathcal{H}(\dot{\phi} + 2\dot{\psi}) + (2\dot{\mathcal{H}} + \mathcal{H}^2)\phi - \frac{\beta + \lambda}{2 + \alpha\mathcal{B}} k^2(\dot{\chi} + 2\mathcal{H}\chi) - \frac{\Omega_\gamma}{2a^2}\delta_{[\gamma]} = 0 \,, \tag{131a}$$

$$\phi - \psi - \beta(\dot{\chi} + 2\mathcal{H}\chi) = 0 \,, \tag{131b}$$

$$\ddot{\chi} + 2\mathcal{H}\dot{\chi} + \mathcal{C}^2 k^2 \chi + \left[\dot{\mathcal{H}}(1 - \mathcal{B}) + \mathcal{H}^2(1 + \mathcal{B}) + \frac{3(2 + \alpha\mathcal{B})Y\Omega_{dm}}{2\alpha\, a}\right]\chi$$
$$- \frac{3(2 + \alpha\mathcal{B})Y\Omega_{dm}}{2\alpha\, a} v_{[dm]} - \dot{\phi} - \mathcal{H}(1 + \mathcal{B})\phi - \mathcal{B}\dot{\psi} = 0 \,, \tag{131c}$$

$$\dot{v}_{[dm]} + \mathcal{H} v_{[dm]} + \frac{Y}{1 - Y}(\dot{\chi} + \mathcal{H}\chi) - \frac{\phi}{1 - Y} = 0 \,, \tag{131d}$$

$$\ddot{\delta}_{[\gamma]} + \frac{k^2}{3}\delta_{[\gamma]} + \frac{4k^2}{3}\phi - 4\ddot{\psi} = 0 \,. \tag{131e}$$

A subtle point is the proper choice of the initial conditions for the system (131). These are fixed deep inside the radiation-domination stage when the modes are superhorizon. We consider the initial conditions corresponding to the adiabatic mode. The latter is regular at $\tau \to 0$. Thus we write for small τ:

$$\phi = \phi^{(0)} + \phi^{(1)}\tau \,, \quad \psi = \psi^{(0)} + \psi^{(1)}\tau \,, \quad \delta_{[\gamma]} = \delta^{(0)}_{[\gamma]} + \delta^{(1)}_{[\gamma]}\tau \,, \tag{132a}$$

$$\chi = \chi^{(1)}\tau + \chi^{(2)}\frac{\tau^2}{2} \,, \quad v_{[dm]} = v^{(1)}_{[dm]}\tau \,. \tag{132b}$$

Expanding Eqs. (131) at $\tau \to 0$ we obtain the relations:

$$\delta^{(0)}_{[\gamma]} = -2\phi^{(0)} \,, \quad \chi^{(1)} = v^{(1)}_{[dm]} = \frac{\phi^{(0)}}{2} \,, \quad \psi^{(0)} = \left(1 - \frac{3\beta}{2}\right)\phi^{(0)} \,, \tag{133a}$$

$$\delta^{(1)}_{[\gamma]} = 4\psi^{(1)} \,, \qquad \phi^{(1)} - \psi^{(1)} - 2\beta\chi^{(2)} - \frac{\beta(\Omega_{dm} + \Omega_b)}{4\sqrt{\Omega_\gamma}}\phi^{(0)} = 0 \,, \tag{133b}$$

$$(2 + \mathcal{B})\phi^{(1)} + \mathcal{B}\psi^{(1)} - (3 + \mathcal{B})\chi^{(2)} - \frac{\Omega_{dm} + \Omega_b}{4\sqrt{\Omega_\gamma}}\phi^{(0)} = 0 \,, \tag{133c}$$

where we have used the expansion of the scale factor at the radiation-domination epoch including the subleading order

$$a = \sqrt{\Omega_\gamma}\tau + \frac{\Omega_{dm} + \Omega_b}{4}\tau^2 \,.$$

Note that Eqs. (133a) describing the leading form of the adiabatic mode agree with those of Sec. 5.1. Additionally, the initial data must satisfy the constraint following from the (00)

Einstein's equation (91a)[25]. This gives,

$$3\psi^{(1)} + \phi^{(1)} + \frac{\Omega_{dm}+\Omega_b}{\sqrt{\Omega_\gamma}}\phi^{(0)} + \frac{\Omega_{dm}}{2\sqrt{\Omega_\gamma}}\delta^{(0)}_{[dm]} + \frac{\Omega_b}{2\sqrt{\Omega_\gamma}}\delta^{(0)}_{[b]} = 0 \ ,$$

where $\delta^{(0)}_{[dm]}$, $\delta^{(0)}_{[b]}$ are the constant terms in the expansion of the DM and baryon density contrasts. For the adiabatic mode we have:

$$\delta^{(0)}_{[dm]} = \delta^{(0)}_{[b]} = \frac{3}{4}\delta^{(0)}_{[\gamma]} \ .$$

Using this relation we obtain for the coefficients of the subleading terms in (132),

$$\phi^{(1)} = \psi^{(1)} = \frac{\delta^{(1)}_{[\gamma]}}{4} = \frac{\chi^{(2)}}{2} = -\frac{\Omega_{dm}+\Omega_b}{16\sqrt{\Omega_\gamma}}\phi^{(0)} \ . \tag{134}$$

In this way all initial conditions for the system (131) are fixed in terms of the overall amplitude $\phi^{(0)}$.

Once the quantities entering the system (131) are computed, we find the DM and baryon density contrasts by integrating the equations

$$\dot{\delta}_{[dm]} + k^2 v_{[dm]} - 3\dot{\psi} = 0 \ , \tag{135a}$$

$$\dot{v}_{[b]} + \mathcal{H} v_{[b]} - \phi = 0 \ , \quad \dot{\delta}_{[b]} + k^2 v_{[b]} - 3\dot{\psi} = 0 \tag{135b}$$

with the initial conditions

$$v_{[b]} = \frac{\phi^{(0)}}{2}\tau \ , \qquad \delta_{[dm]} = \delta_{[b]} = -\frac{3}{2}\phi^{(0)} \ .$$

By similar reasoning we also obtain the equations and initial conditions for the case of ΛCDM. As we are interested in comparing the evolution of perturbations in the proposed model and ΛCDM we can choose arbitrary normalization for $\phi^{(0)}$, the only requirement being that this normalization is the same for the computations in both models. In practice we take $\phi^{(0)} = 1$ to compute the transfer functions which we multiply by a flat initial spectrum when appropriate.

References

[1] V. A. Kostelecky and N. Russell, Rev. Mod. Phys. **83**, 11 (2011) [arXiv:0801.0287 [hep-ph]].

[2] S. Weinberg, Phys. Rev. **138**, B988 (1965).

[25] It is straightforward to check that the $(0i)$ equation (91b) does not produce any new constraints.

[3] S. Deser, Gen. Rel. Grav. **1**, 9 (1970) [gr-qc/0411023].

[4] R. M. Wald, Phys. Rev. D **33**, 3613 (1986).

[5] D. Blas, J. Phys. A A **40**, 6965 (2007) [hep-th/0701049].

[6] P. Horava, Phys. Rev. D **79**, 084008 (2009) [arXiv:0901.3775 [hep-th]].

[7] D. Blas, O. Pujolas and S. Sibiryakov, Phys. Lett. B **688**, 350 (2010) [arXiv:0912.0550 [hep-th]].

[8] D. Mattingly, Living Rev. Rel. **8**, 5 (2005) [gr-qc/0502097].

[9] T. Jacobson, S. Liberati and D. Mattingly, Annals Phys. **321**, 150 (2006) [astro-ph/0505267].

[10] D. Blas, O. Pujolas and S. Sibiryakov, JHEP **0910**, 029 (2009) [arXiv:0906.3046 [hep-th]].

[11] T. Jacobson and D. Mattingly, Phys. Rev. D **64**, 024028 (2001) [arXiv:gr-qc/0007031].

[12] T. Jacobson, PoS **QG-PH**, 020 (2007) [arXiv:0801.1547 [gr-qc]].

[13] B. Withers, Class. Quant. Grav. **26**, 225009 (2009) [arXiv:0905.2446 [gr-qc]].

[14] D. Blas, O. Pujolas, S. Sibiryakov, JHEP **1104**, 018 (2011). [arXiv:1007.3503 [hep-th]].

[15] T. Jacobson, Phys. Rev. D **81**, 101502 (2010) [Erratum-ibid. D **82**, 129901 (2010)] [arXiv:1001.4823 [hep-th]].

[16] D. Blas, O. Pujolas and S. Sibiryakov, Phys. Rev. Lett. **104** (2010) 181302 [arXiv:0909.3525 [hep-th]].

[17] S. Mukohyama, Class. Quant. Grav. **27**, 223101 (2010) [arXiv:1007.5199 [hep-th]].

[18] D. Blas and H. Sanctuary, Phys. Rev. D **84** (2011) 064004 [arXiv:1105.5149 [gr-qc]].

[19] S. Groot Nibbelink and M. Pospelov, Phys. Rev. Lett. **94**, 081601 (2005) [arXiv:hep-ph/0404271]. P. A. Bolokhov, S. G. Nibbelink and M. Pospelov, Phys. Rev. D **72**, 015013 (2005) [arXiv:hep-ph/0505029].

[20] O. Pujolas and S. Sibiryakov, JHEP **1201**, 062 (2012) [arXiv:1109.4495 [hep-th]].

[21] M. Pospelov and Y. Shang, Phys. Rev. D **85**, 105001 (2012) [arXiv:1010.5249 [hep-th]].

[22] D. Blas, S. Sibiryakov, JCAP **1107**, 026 (2011) [arXiv:1104.3579 [hep-th]].

[23] L. D. Duffy and K. van Bibber, New J. Phys. **11**, 105008 (2009) [arXiv:0904.3346 [hep-ph]].

[24] J. A. Frieman and B. -A. Gradwohl, Phys. Rev. Lett. **67** (1991) 2926.

[25] B. -A. Gradwohl and J. A. Frieman, Astrophys. J. **398** (1992) 407.

[26] J. Bovy and G. R. Farrar, Phys. Rev. Lett. **102**, 101301 (2009) [arXiv:0807.3060 [hep-ph]].

[27] S. M. Carroll, S. Mantry, M. J. Ramsey-Musolf and C. W. Stubbs, Phys. Rev. Lett. **103**, 011301 (2009) [arXiv:0807.4363 [hep-ph]]; S. M. Carroll, S. Mantry and M. J. Ramsey-Musolf, Phys. Rev. D **81**, 063507 (2010) [arXiv:0902.4461 [hep-ph]].

[28] J. W. Elliott, G. D. Moore and H. Stoica, JHEP **0508**, 066 (2005) [hep-ph/0505211].

[29] S. Dubovsky, T. Gregoire, A. Nicolis and R. Rattazzi, JHEP **0603**, 025 (2006) [arXiv:hep-th/0512260].

[30] A. Adams, N. Arkani-Hamed, S. Dubovsky, A. Nicolis and R. Rattazzi, JHEP **0610**, 014 (2006) [hep-th/0602178].

[31] D. Blas and S. Sibiryakov, Phys. Rev. D **84** (2011) 124043 [arXiv:1110.2195 [hep-th]].

[32] S. M. Carroll and E. A. Lim, Phys. Rev. D **70**, 123525 (2004) [arXiv:hep-th/0407149].

[33] B. Z. Foster and T. Jacobson, Phys. Rev. D **73** (2006) 064015 [gr-qc/0509083].

[34] C. M. Will, Living Rev. Rel. **9**, 3 (2005) [arXiv:gr-qc/0510072].

[35] C. M. Will, "Theory and experiment in gravitational physics," *Cambridge, UK: Univ. Pr. (1993), 380 p.*

[36] B. Z. Foster, Phys. Rev. D **73**, 104012 (2006) [Erratum-ibid. D **75**, 129904 (2007)] [gr-qc/0602004]; Phys. Rev. D **76**, 084033 (2007) [arXiv:0706.0704 [gr-qc]].

[37] S. Liberati and D. Mattingly, "Lorentz breaking effective field theory models for matter and gravity: theory and observational constraints," arXiv:1208.1071 [gr-qc].

[38] S. R. Coleman and S. L. Glashow, Phys. Rev. D **59**, 116008 (1999) [hep-ph/9812418].

[39] I. Carruthers and T. Jacobson, Phys. Rev. D **83**, 024034 (2011) [arXiv:1011.6466 [gr-qc]].

[40] J. Khoury and A. Weltman, Phys. Rev. Lett. **93**, 171104 (2004) [astro-ph/0309300].

[41] N. Andersson and G. L. Comer, Living Rev. Rel. **10** (2005) 1 [gr-qc/0605010].

[42] C. Armendariz-Picon, N. F. Sierra and J. Garriga, JCAP **1007** (2010) 010 [arXiv:1003.1283 [astro-ph.CO]].

[43] C. -P. Ma and E. Bertschinger, Astrophys. J. **455**, 7 (1995) [astro-ph/9506072].

[44] T. P. Sotiriou and V. Faraoni, Rev. Mod. Phys. **82**, 451 (2010) [arXiv:0805.1726 [gr-qc]].

[45] G. R. Dvali, G. Gabadadze and M. Porrati, Phys. Lett. B **485**, 208 (2000) [hep-th/0005016].

[46] S. Tsujikawa, Lect. Notes Phys. **800**, 99 (2010) [arXiv:1101.0191 [gr-qc]].

[47] G. R. Farrar and P. J. E. Peebles, Astrophys. J. **604**, 1 (2004) [astro-ph/0307316].

[48] S. S. Gubser and P. J. E. Peebles, Phys. Rev. D **70**, 123510 (2004) [hep-th/0402225]; Phys. Rev. D **70**, 123511 (2004) [hep-th/0407097].

[49] G. R. Farrar and R. A. Rosen, Phys. Rev. Lett. **98**, 171302 (2007) [astro-ph/0610298].

[50] R. Bean, E. E. Flanagan, I. Laszlo and M. Trodden, Phys. Rev. D **78**, 123514 (2008) [arXiv:0808.1105 [astro-ph]].

[51] J. A. Keselman, A. Nusser and P. J. E. Peebles, Phys. Rev. D **81** (2010) 063521 [arXiv:0912.4177 [astro-ph.CO]].

[52] L. Amendola, Phys. Rev. D **69**, 103524 (2004) [astro-ph/0311175].

[53] R. Scoccimarro, Phys. Rev. D **80** (2009) 104006 [arXiv:0906.4545 [astro-ph.CO]].

[54] F. Saracco, M. Pietroni, N. Tetradis, V. Pettorino and G. Robbers, Phys. Rev. D **82**, 023528 (2010) [arXiv:0911.5396 [astro-ph.CO]].

[55] P. Brax and P. Valageas, "Structure Formation in Modified Gravity Scenarios," arXiv:1205.6583 [astro-ph.CO].

[56] M. Kesden and M. Kamionkowski, Phys. Rev. D **74** (2006) 083007 [astro-ph/0608095].